Bosonic corrections to Δr at the two-loop level

M. Awramik,[1,2] M. Czakon,[2,3] A. Onishchenko,[1,4] and O. Veretin[1]
[1]*Institut für Theoretische Teilchenphysik, Universität Karlsruhe, D-76128 Karlsruhe, Germany*
[2]*Department of Field Theory and Particle Physics, Institute of Physics, University of Silesia, Uniwersytecka 4, PL-40007 Katowice, Poland*
[3]*Institut für Theoretische Physik, Universität Karlsruhe, D-76128 Karlsruhe, Germany*
[4]*State Research Center, Institute for High Energy Physics, Protvino, Moscow Region, 142284 Russia*
(Received 11 December 2002; published 23 September 2003)

The details of two recent calculations of the two-loop bosonic corrections to the muon lifetime in the standard model are presented. The matching to the Fermi theory is discussed. Renormalization in the on-shell and the modified minimal subtraction schemes is studied and the transition between the schemes is shown to lead to identical results. High precision numerical methods are compared with the mass difference and large mass expansions.

DOI: 10.1103/PhysRevD.68.053004 PACS number(s): 12.15.Lk, 13.35.Bv, 14.60.Ef

I. INTRODUCTION

The muon decay lifetime (τ_μ) has been used for a long time as an input parameter for high precision predictions of the standard model (SM). It allows for an indirect determination of the mass of the W boson (M_W), which suffers currently from a large experimental error of 39 MeV [1], one order of magnitude worse than that of the Z boson mass (M_Z). A reduction of this error by the CERN Large Hadron Collider (LHC) to 15 MeV [2] and by a future linear collider to 6 MeV [3] would provide a stringent test of the SM by confronting the theoretical prediction with the experimental value.

The extraction of M_W with an accuracy matching that of the next experiments, i.e., at the level of a few MeV, necessitates radiative corrections beyond one-loop order. Large two-loop contributions from fermionic loops have been calculated in [4]. The current prediction is affected by two types of uncertainties. First, apart from the still unknown Higgs boson mass, two input parameters introduce large errors. The current knowledge of the top quark mass results in an error of about 30 MeV [5], which should be reduced by the LHC to 10 MeV and by a linear collider even down to 1.2 MeV. The inaccuracy of the knowledge of the running of the fine structure constant up to the M_Z scale, $\Delta\alpha(M_Z)$, introduces a further 6.5 MeV error. Second, several higher order corrections are unknown. In fact the last unknown correction at the $O(\alpha^2)$ order has been calculated only recently in [6] and [7]. This contribution comes from diagrams with no closed fermion loops.

It is the purpose of the present work to give a detailed description of the methods used in the calculations presented in [6] and [7]. Since one of the groups used high precision numeric methods and the other deep expansions both in mass differences and in large masses, a comparison can be given.

In the next section we discuss the question of matching of the Fermi theory onto the standard model at low energy scales. Then we move to a discussion of renormalization in the on-shell scheme and continue with the modified minimal subtraction ($\overline{\text{MS}}$) scheme. A section on the transition between the schemes contains comparisons of the methods and the final results. A description of the computational methods and conclusions close the main part of the work. In the Appendixes, a derivation of the electric charge counterterm through the $U(1)$ Ward identity can be found, followed by the explicit analytic results for the expansions of the on-shell and $\overline{\text{MS}}$ quantities.

II. MATCHING

The muon lifetime τ_μ can be computed from the effective Fermi theory given by the Lagrangian

$$\mathcal{L}^{\text{eff}} = \mathcal{L}_{\text{QED}} + \mathcal{L}^{(5)}_{\text{QCD}} + \frac{G_F}{\sqrt{2}} O_F + \text{higher dimension operators}, \tag{1}$$

where O_F is the four-fermion Fermi operator of dimension 6:

$$O_F = [\bar{\nu}_\mu \gamma^\alpha (1-\gamma_5)\mu][\bar{e}\gamma_\alpha(1-\gamma_5)\nu_e], \tag{2}$$

and G_F is the Fermi constant. Note that Eq. (1) is a definition of G_F. This Lagrangian can be used to describe low energy processes (such that energies are $\ll M_W$) mediated by the weak charged current. Since the theory of Eq. (1) is nonrenormalizable, an ultraviolet cutoff Λ should be introduced.

In particular, for the muon decay process we have

$$\frac{1}{\tau_\mu} = \frac{G_F^2 m_\mu^5}{192\pi^3}\left(1 - 8\frac{m_e^2}{m_\mu^2}\right)(1+\Delta q), \tag{3}$$

with m_e and m_μ being the masses of the electron and the muon, respectively. The quantity Δq describes all QED corrections in the Fermi theory and has been calculated at the one-loop [8] and the two-loop [9] order.

By its nature G_F is the Wilson coefficient function of the operator O_F and can be evaluated from the SM. Traditionally, the matching relation between G_F and the parameters of the SM is parametrized as follows:

$$\frac{G_F}{\sqrt{2}}=\frac{e^2}{8(1-M_W^2/M_Z^2)M_W^2}(1+\Delta r). \tag{4}$$

The quantity $\Delta r=\Delta r^{(1)}+\Delta r^{(2)}+\cdots$ absorbs the effects of all loop diagrams.

It is the purpose of the following subsection to establish the framework for the calculation of Δr.

A. Factorization theorem

In principle, the muon decay amplitude can be evaluated directly in the SM, but this is not feasible in practice. There are many scales involved which vary from less than 1 MeV to 100 GeV, i.e., by more than five orders of magnitude. On the other hand, the number of Feynman diagrams grows very fast with the number of loops. A way to keep the problem manageable is to switch on the machinery of effective Lagrangians [see Eq. (1)]. This allows one to simplify the calculation enormously and to separate consistently the low energy (''soft'') dynamics from the high energy (''hard'') static characteristics.

Suppose that we can compute the muon decay amplitude $A^{\rm SM}$ in the SM. Then the Fermi constant G_F defined through Eq. (1) can be predicted from $A^{\rm SM}$. Indeed, we should require that both evaluations in the SM and the Fermi theory give the same result. At the tree level the corresponding matching equation reads

$$A^{\rm SM}=\frac{G_F}{\sqrt{2}}\langle\mu|O_F|e\,\nu_\mu\overline{\nu_e}\rangle+O\left(\frac{m_\mu^4}{M_W^4}\right). \tag{5}$$

This equation just states that the amplitude of the process $\mu\to e\,\nu\overline{\nu}$ is the same both in the full SM and in the effective Fermi theory up to operators of higher dimension.

When loop effects are taken into account, matrix elements in both sides of Eq. (5) get quantum corrections. Since $A^{\rm SM}$ and $\langle\mu|O_F|e\,\nu_\mu\overline{\nu_e}\rangle$ are amputated matrix elements one has to renormalize the external wave functions also. Therefore the final form of the matching equation reads

$$\begin{aligned}&\sqrt{Z_{2,e}^{\rm SM}Z_{2,\mu}^{\rm SM}Z_{2,\nu_e}^{\rm SM}Z_{2,\nu_\mu}^{\rm SM}}\;A^{\rm SM}\\&=\sqrt{Z_{2,e}^{\rm eff}Z_{2,\mu}^{\rm eff}Z_{2,\nu_e}^{\rm eff}Z_{2,\nu_\mu}^{\rm eff}}Z_{O_F}^{-1}\frac{G_F}{\sqrt{2}}\langle\mu|O_F|e\,\nu_\mu\overline{\nu_e}\rangle\\&\quad+O\left(\frac{m_\mu^4}{M_W^4}\right),\end{aligned} \tag{6}$$

where $Z_{2,f}^{\rm SM}$ and $Z_{2,f}^{\rm eff}$ are the wave function renormalization constants of the fermions evaluated in the SM and in the effective theory, respectively, and Z_{O_F} is the renormalization constant of the Fermi operator in the effective theory.

There are two ways to compute G_F from the SM: (1) a standard matching calculation, or (2) automatic matching via the factorization theorem.

The former approach works always by simply computing all ingredients (apart from G_F) in the matching equation Eq. (6). This requires, however, much extra effort to evaluate the ''soft'' pieces (or, at least, to separate them) in the amplitudes and the Z's. Historically, for this purpose the Pauli-Villars regularization was used in [10] and then extended to two-loop order in [11]. The same approach has also been applied in [5].

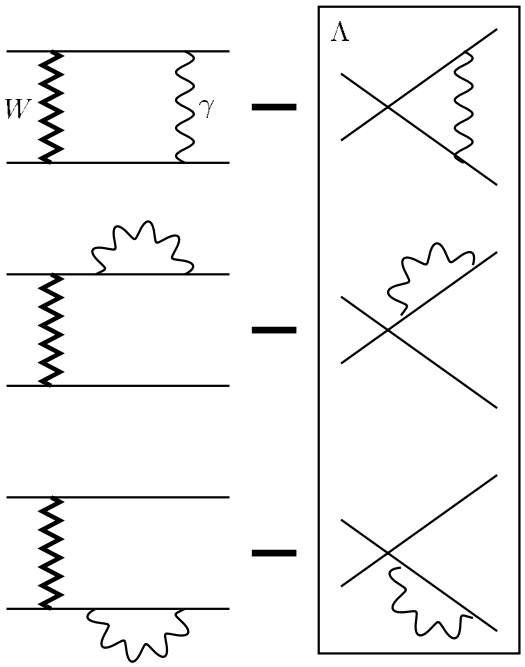

FIG. 1. One-loop factorization with Pauli-Villars regularization.

How it works at the one-loop level is demonstrated in Fig. 1. There are only three infrared divergent diagrams with a photon. From each diagram its counterpart in the Fermi theory should be subtracted. The left diagram in each line of Fig. 1 corresponds to the result in the full model and therefore contains both the ''soft'' and the ''hard'' parts. The right one contains only the ''soft'' part, which means that the difference is the requested ''hard'' correction. In addition, for the diagrams in the frame the Pauli-Villars regularization is introduced to regularize the ultraviolet divergences. At the two-loop level we have a very similar situation. The difference is that instead of ''hard'' and ''soft'' terms there are now ''hard-hard,'' ''hard-soft,'' ''soft-hard,'' and ''soft-soft'' contributions. Of these, only the ''hard-hard'' piece contributes to G_F.

Accidentally, it happens that the sum of the three ''soft'' diagrams inside the frame in Fig. 1 is an ultraviolet finite quantity (let us call it $\Sigma_{\rm soft}$). It is easy to prove that this holds true also to all orders. This is a consequence of the Ward-Takahashi identity for QED. This fact, however, is a pure coincidence rather than something fundamental. If such a cancellation had not occurred, renormalization of the operator O_F would be required, as is taken into account in Eq. (6).

The scheme given in Fig. 1 is consistent but the disadvantage of it is that there arises the problem of bookkeeping of ''soft'' and ''hard'' parts, and the problem is already very complicated at the two-loop level. Indeed, at the two-loop level one has to subtract from each diagram the ''hard-soft,'' ''soft-hard,'' and ''soft-soft'' pieces.

Therefore it would be very helpful to find some other way to obtain the ''hard'' part. Thus we come to the second way to compute G_F—automatic matching. This procedure is the most straightforward and the most economical (minimal in cost) way to compute. It is based on the factorization theorem, proven, e.g., in [12]. It allows one to extract the ''hard'' part directly without any reference to ''soft'' pieces. As a well known example of such a procedure we can mention the evaluation of Wilson coefficient functions in deep inelastic scattering processes.

Returning to the sum of the three ''soft'' graphs in Fig. 1 ($\Sigma_{\rm soft}$) we notice that in G_F all ''soft'' modes are eliminated. This means that all subgraphs in Fig. 1 should be computed at vanishing masses of the leptons. In this case the Ward-Takahashi identity not only makes $\Sigma_{\rm soft}$ ultraviolet finite but also nullifies it. Thus all ''soft'' parts add up to zero. This is also true to all orders of perturbation theory. In other words, one can from the very beginning nullify all external momenta and masses and evaluate the bubble diagrams obtained. Of course, new infrared divergences are generated. They cancel, however, in the expression for G_F. To regularize these infrared divergences we use the dimensional regularization.

To prove rigorously that infrared singularities indeed drop out from the result one can turn to the framework for construction of effective low energy Lagrangians given in [12]. At the level of individual Feynman diagrams one can separate ''soft'' and ''hard'' scales with the help of the asymptotic expansion procedure [13]. Let F denote a Feynman diagram. Then

$$F \sim \sum_{H \subseteq F} S \cdot T(H), \tag{7}$$

where the sum runs over all ''hard'' subgraphs H of the diagram F; S is a ''soft'' subgraph obtained from F by shrinking H to a point and T stands for the Taylor expansion (before integration) of H with respect to all ''soft'' parameters. The exact rules for construction of hard subgraphs are discussed in detail in [13].

The important property of the operation Eq. (7) is that it has the combinatorial structure of the R operation [14]. This allows one to promote the operation on a single Feynman diagram to an operation on the whole Feynman amplitude (the factorization theorem). By this procedure all infrared divergencies are absorbed either by the ''soft'' matrix element or by the renormalization constant Z_O of the operator. The detailed discussion can be found in [12]. At this point, we should stress once more that although in general the separation into ''soft'' and ''hard'' parts is arbitrary, in this case it is fixed by the existing result for the QED corrections in the Fermi model [8,9], and the procedure described above satisfies the appropriate matching equation, Eq. (5).

In the case of G_F we have further simplifications:

(1) The anomalous dimension of the Fermi operator O_F is zero; therefore Z_{O_F} in the matching equation Eq. (6) is equal to 1.

(2) At zero lepton masses and external momenta all $Z_2^{\rm eff}$ and the ''soft'' matrix element in Eq. (6) are equal to 1.

Finally we get

$$\frac{G_F}{\sqrt{2}} = [\sqrt{Z_{2,e}^{\rm SM} Z_{2,\mu}^{\rm SM} Z_{2,\nu_e}^{\rm SM} Z_{2,\nu_\mu}^{\rm SM}}\ A^{\rm SM}]_{\rm hard}, \tag{8}$$

where the subscript ''hard'' means that all ''soft'' scales are put to zero.

Thus the problem is reduced completely to the vacuum Feynman diagrams of one- and two-loop order and the bookkeeping problem does not arise at all. The wave function renormalization constants are to be computed in the on-shell scheme. Again, for massless leptons, the wave function renormalization constants are defined through vacuum diagrams only. Such diagrams can be evaluated analytically using the reduction formulas of [15] based on Integration by Parts identities [16].

B. Projection

An important problem in the calculation is the reduction of the amplitudes to scalar integrals. It is not only of practical importance. In fact, it is connected to the correct definition of the matrix elements in the model, since dimensional regularization is used.

The matching to the Fermi theory with its double V-A chiral structure is made possible because of the left-handedness of the charged current in the standard model. The ''hard'' components of the diagrams contain only massless fermions and therefore formally the structure of the two spinor lines can be mapped onto the operator

$$\gamma^\mu P_L \otimes \gamma_\mu P_L. \tag{9}$$

In four dimensions, every string of an odd number of gamma matrices and a left-handed projector can be reduced to the structure $\gamma^\mu P_L$ due to the Chisholm identity

$$\gamma_\mu \gamma_\nu \gamma_\rho = g_{\mu\nu}\gamma_\rho + g_{\nu\rho}\gamma_\mu - g_{\mu\rho}\gamma_\nu - i\epsilon_{\mu\nu\rho\sigma}\gamma^\sigma\gamma_5. \tag{10}$$

The reduction leads to the operator

$$T_{\mu\nu}\gamma^\mu P_L \otimes \gamma^\nu P_L, \tag{11}$$

where $T_{\mu\nu}$ is some tensor made of the integration momenta. Since there are no nonvanishing external momenta, this tensor must be proportional to $g_{\mu\nu}$ and the result Eq. (9) follows. A suitable way to obtain the right value directly is to use a projector made of trace operators. Let the original product of strings of gamma matrices be denoted by

$$\Gamma_1 \otimes \Gamma_2. \tag{12}$$

We wish to obtain the proportionality coefficient A in the following equation:

$$\int \Gamma_1 \otimes \Gamma_2 = A \times (\gamma^\mu P_L \otimes \gamma_\mu P_L). \tag{13}$$

Two possibilities of closing the spinor strings with trace operators are depicted in Fig. 2. The left one has been used in [5] and is given by the equation

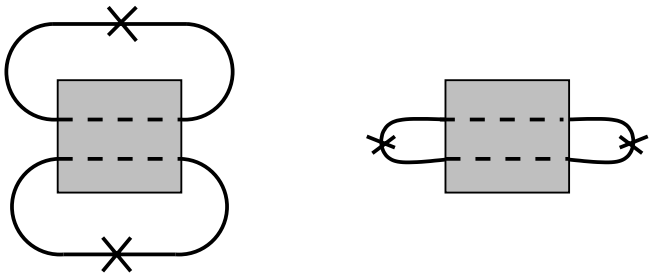

FIG. 2. Two of the possible projectors for Δr. The dashed lines represent the strings of Dirac matrices, and the crosses the projection operators.

$$A=\frac{1}{4d}\int \mathrm{Tr}(\Gamma_1\gamma^\mu P_R)\mathrm{Tr}(\Gamma_2\gamma_\mu P_R), \tag{14}$$

where the dimension of space-time d has been kept arbitrary and the trace of the unit matrix has been put to 4, as usual. A second possibility which we used to perform the calculations presented in this work is given by

$$A=-\frac{1}{2d(d-2)}\int \mathrm{Tr}(\Gamma_1\gamma_\mu P_R\Gamma_2\gamma^\mu P_R), \tag{15}$$

and corresponds to the right picture in Fig. 2.

Both projectors are obviously equivalent in four dimensions due to the Chisholm identity as explained above. The difference starts to be important for divergent integrals. In fact the problem only occurs for one-particle-irreducible four-point diagrams, where the divergence can come from two sources: first from the external wave function renormalization, which is incomplete due to infrared divergences, and second due to infrared divergences of the diagrams themselves. As noticed in [5] the first projector Eq. (14) needs to be corrected, as it does not satisfy several requirements, like, for example, the vanishing of diagrams with propagator insertion in the photon lines. Moreover, one can explicitly check that without corrections the subtracted diagrams in the Pauli-Villars approach do not cancel and the dependence on the Λ scale remains. In the automatic factorization approach this shows up through an incomplete cancellation of divergences. Notice, however, that the result is gauge independent; thus it is only the finiteness of the result that shows that the projector is incorrect.

On the contrary, the projector Eq. (15) does not require any corrections. It does satisfy all the algebraic requirements and also yields a finite result as well as the exact cancellation of the subtraction diagrams of Fig. 1 in d dimensions and in all orders of perturbation theory. This useful property follows from the fact that this projector respects the Fierz symmetry in d dimensions with respect to the last vector boson line connecting the two gamma matrix strings. One can check explicitly that, for example,

$$\gamma_\mu\gamma_\nu\gamma_\rho P_L\otimes\gamma^\rho\gamma^\nu\gamma^\mu P_L\sim\gamma_\mu\gamma_\nu\gamma_\rho\gamma^\nu\gamma^\mu P_L\otimes\gamma^\rho P_L, \tag{16}$$

where $\sim$ means equality after projection. In fact, if the fermion strings of Eq. (12) are rewritten as

$$\Gamma_1=\Gamma_1'\gamma^\mu P_L, \tag{17}$$

$$\Gamma_2=\gamma_\mu P_L\Gamma_2', \tag{18}$$

then the projector will give the same result for

$$\Gamma_1'\gamma^\mu P_L\otimes\gamma_\mu P_L\Gamma_2' \tag{19}$$

and

$$\Gamma_1'\gamma^\mu P_L\Gamma_2'\otimes\gamma_\mu P_L, \tag{20}$$

which can be proved by inserting both expressions into Eq. (15) and performing the trivial index contraction.

III. ON-SHELL RENORMALIZATION

Two-loop calculations within the on-shell renormalization scheme require the knowledge of several counterterms. At the very least, charge and mass counterterms are needed. In this section we first discuss the problem of gauge invariance in connection with tadpole diagrams. We then give specific expressions for the required counterterms.

A. Tadpoles and gauge invariance of counterterms

It has been known for a long time that the inclusion of tadpoles is necessary to obtain gauge invariant counterterms. In fact, this property was first noticed [17,18] shortly after the proof of renormalizability of gauge theories, and explicit calculations have shown how this works up to the two-loop level [19]. A general proof of the quantum action principle, which has as a consequence the gauge invariance of on-shell processes in the bare Lagrangian, requires the inclusion of even those tadpoles that would be cancelled by normal ordering (one-loop tadpoles) [20]. There are, however, two disadvantages of having tadpoles in actual calculations. First, this requires the inclusion of diagrams that dropout in the final result. Second, in large scale calculations one would like to reduce the number of diagrams as much as possible by evaluating only the one-particle-irreducible (1PI) ones, and these cannot have tadpole parts. Therefore, as long as we wish to obtain results at the least cost and by using automated software, it is interesting to consider alternative possibilities.

It turns out that it is possible to prepare the bare Lagrangian in such a way, that the only gauge dependent quantities would be the wave function renormalization constants and the vacuum renormalization constant, and still all of the tadpoles would be canceled [17]. Let us start by considering a Lagrangian in which the bare coupling and masses are defined through physical processes. The masses can be equivalently defined through the position of the poles of the physical S matrix in the complex plane as recently proved [21]. In such a case all of the bare parameters would be gauge invariant, because they would satisfy equations that have this same property (as long as they are given in an invariant regularization, of course). It is important to supply a condition on the vacuum expectation value of the bare Higgs field v_0 that would resum terms of order $O(\alpha^0)$. A choice that is still

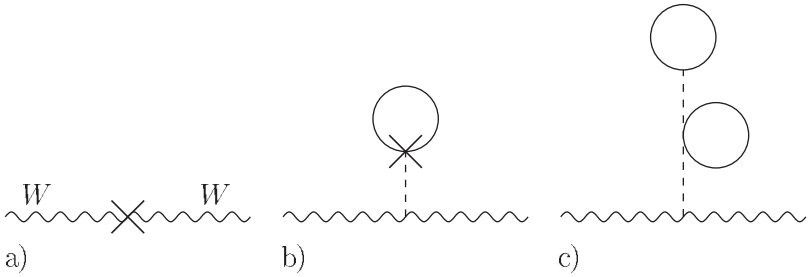

FIG. 3. Vacuum expectation value counterterm insertion into the W boson self-energy (a), reproducing tadpole insertions (b) and (c).

consistent with gauge invariance is

$$\frac{1}{2}v_0\left(\frac{1}{2}v_0^2\lambda_0-\mu_0^2\right)=0, \tag{21}$$

where λ_0 and μ_0 are defined through the Higgs Lagrangian

$$\mathcal{L}_{\text{Higgs}}=\frac{1}{2}\mu_0^2\Phi_0^\dagger\Phi_0-\frac{1}{4}\lambda_0(\Phi_0^\dagger\Phi_0)^2, \tag{22}$$

and Φ_0 is the Higgs doublet. Equation (21) implies the vanishing of the linear term in the Lagrangian. Although this term will be subsequently altered, the tree-level contribution will always vanish.

We now introduce an additional renormalization of the bare vacuum expectation value

$$v_0\to v_0 Z_v^{1/2}. \tag{23}$$

The renormalization constant Z_v can be used to cancel the tadpoles recursively, which implies together with Eq. (21) that the first nonvanishing term in its perturbative expansion starts at order $O(\alpha)$. The linear term in the Higgs field can now be written as

$$-T_0H^0=-\frac{M_W^0\sin\theta_W^0}{e_0}(M_H^0)^2Z_v^{1/2}(Z_v-1)H^0, \tag{24}$$

where the following relations have been used:

$$v_0=\frac{2\sin\theta_W^0M_W^0}{e_0}, \tag{25}$$

$$\mu_0^2=(M_H^0)^2, \tag{26}$$

$$\lambda_0=\left(\frac{e_0M_H^0}{\sin\theta_W^0M_W^0}\right)^2. \tag{27}$$

At the tree level the contribution is zero, since then $Z_v^{(0)}=1$, as noticed above. To one-loop order, the relation between the tadpole diagrams and the vacuum expectation value is simple:

$$\delta Z_v^{(1)}=\frac{e}{\sin\theta_WM_WM_H^2}\Pi_H^{(1)}, \tag{28}$$

where $i\Pi_H^{(1)}$ is the sum of 1PI one-loop tadpole diagrams of the Higgs field. The situation gets much more complicated at the two-loop level:

$$\delta Z_v^{(2)}=\frac{e}{\sin\theta_WM_WM_H^2}\Pi_H^{(2)}-\frac{1}{2}\delta Z_v^{(1)}\left(\delta Z_v^{(1)}+\delta Z_H^{(1)}+2\frac{\delta M_H^{2(1)}}{M_H^2}+\frac{\delta M_W^{2(1)}}{M_W^2}+2\frac{\delta\sin\theta_W^{(1)}}{\sin\theta_W}-\delta Z_e^{(1)}\right). \tag{29}$$

The insertion of this counterterm reproduces all of the tadpole diagrams that would be included in the usual approach. An example is depicted in Fig. 3. A Z_v in the W boson self-energy (a) leads effectively through the first term in Eq. (29) to insertion of a one-loop tadpole with a vertex counterterm (b). This counterterm also contains a correction to the vacuum expectation value of the Higgs field, which reproduces the tadpole diagram (c).

B. On-shell scheme counterterms

The on-shell renormalization scheme is defined by the requirement that the masses be identified through the poles of the physical S matrix (as the real part of the pole), while the electric charge coincides with the value measured in the Thompson scattering process, as for example in the quantum Hall effect. These conditions are enough to fix all of the free parameters of the SM with minimal Higgs sector [neglecting the Cabibbo-Kobayashi-Maskawa (CKM) matrix and the strong coupling constant]. The counterterms have been given by many authors (although here we need also to supply the ϵ order parts at the one-loop level). The peculiarity of the present work is the specific definition of the bare masses, which are gauge invariant without including tadpole diagrams. This, however, implies that the formulas defining the counterterms will be slightly different.

At the one-loop level, the mass counterterms are related to the on-shell self-energies through

$$\delta M_H^{2(1)}=\text{Re}\Pi_{HH}^{(1)}(M_H^2)-\frac{3}{2}M_H^2\delta Z_v^{(1)}, \tag{30}$$

$$\delta M_W^{2(1)}=-\Pi_{WW,T}^{(1)}(M_W^2)-M_W^2\delta Z_v^{(1)}, \tag{31}$$

$$\delta M_Z^{2(1)}=-\Pi_{ZZ,T}^{(1)}(M_Z^2)-M_Z^2\delta Z_v^{(1)}, \tag{32}$$

where $i\Pi_{ii}$ denotes the self-energy diagrams of the boson i and the subscript T stands for the transverse part. For bosonic corrections to the Higgs boson mass counterterm the real part has to be taken due to the possible decay into a W or Z boson pair. To one-loop order this still yields a gauge invariant

result for the renormalized amplitude. The W and Z bosons do not require such a treatment either at one- or at two-loop order.

At the two-loop order, only W and Z boson mass counterterms are needed, and they assume the form

$$\delta M_W^{2(2)} = -\Pi_{WW,T}^{(2)}(M_W^2) - \delta Z_W^{(1)} \delta M_W^{2(1)} - M_W^2 \delta Z_v^{(2)} - \delta Z_v^{(1)} (M_W^2 \delta Z_W^{(1)} + \delta M_W^{2(1)}), \tag{33}$$

$$\delta M_Z^{2(2)} = -\Pi_{ZZ,T}^{(2)}(M_Z^2) - \delta Z_Z^{(1)} \delta M_Z^{2(1)} - M_Z^2 \delta Z_v^{(2)} - \delta Z_v^{(1)} (M_Z^2 \delta Z_Z^{(1)} + \delta M_Z^{2(1)}) + \frac{1}{4} M_Z^2 (\delta Z_{\gamma Z}^{(1)})^2. \tag{34}$$

The last term in the Z boson mass counterterm, which does not occur in the W boson mass counterterm, has its origin in the mixing between Z and γ. If the self-energies have imaginary parts, then suitable additional terms have to be included as described in [5]. The above formulas are valid only if the subdivergencies in the two-loop self-energies are renormalized. They also require the wave function renormalization constants of the bosons (the prime denotes a derivative with respect to the momentum squared)

$$\delta Z_W^{(1)} = \Pi_{WW,T}^{(1)\prime}(M_W^2), \tag{35}$$

$$\delta Z_Z^{(1)} = \Pi_{ZZ,T}^{(1)\prime}(M_Z^2) \tag{36}$$

and the mixing renormalization

$$\delta Z_{\gamma Z}^{(1)} = \frac{2}{M_Z^2} \Pi_{\gamma Z,T}^{(1)}(M_Z^2). \tag{37}$$

The last two constants form part of the 2×2 renormalization matrix of the neutral bosons

$$\begin{pmatrix} A_\mu^0 \\ Z_\mu^0 \end{pmatrix} = \begin{pmatrix} Z_{ZZ}^{1/2} & \frac{1}{2} Z_{\gamma Z} \\ \frac{1}{2} Z_{Z\gamma} & Z_{\gamma\gamma}^{1/2} \end{pmatrix} \begin{pmatrix} A_\mu \\ Z_\mu \end{pmatrix}. \tag{38}$$

The remaining two renormalization constants define the photon field and can be obtained at zero momentum transfer from the following formulas:

$$\delta Z_{Z\gamma}^{(1)} = -\frac{2}{M_Z^2} \Pi_{\gamma Z,T}^{(1)}(0), \tag{39}$$

$$\delta Z_{\gamma\gamma}^{(1)} = \Pi_{\gamma\gamma,T}^{(1)\prime}(0). \tag{40}$$

The electric charge counterterm can be obtained in two ways. The first consists in simply calculating the scattering of fermions off real photons, i.e., at zero momentum transfer. This, however, unnecessarily introduces three-point functions. A second possibility is to use the $U(1)$ Ward identity. A suitable relation between the wave function renormalization constants of the photon and the Z boson was proved in [22,23] using the BRS symmetry. A simpler proof is given in Appendix A. The one- and two-loop counterterms in the on-shell scheme are given by

$$\delta Z_e^{(1)} = -\frac{1}{2} \delta Z_{\gamma\gamma}^{(1)} - \frac{1}{2} \frac{\sin\theta_W}{\cos\theta_W} \delta Z_{Z\gamma}^{(1)}, \tag{41}$$

$$\delta Z_e^{(2)} = -\frac{1}{2} \delta Z_{\gamma\gamma}^{(2)} - \frac{1}{2} \frac{\sin\theta_W}{\cos\theta_W} \delta Z_{Z\gamma}^{(2)} + (\delta Z_e^{(1)})^2 + \frac{1}{8} (\delta Z_{\gamma\gamma}^{(1)})^2 - \frac{1}{2} \frac{\delta \sin\theta_W}{\cos^3\theta_W} \delta Z_{Z\gamma}^{(1)}. \tag{42}$$

The two-loop wave function renormalization of the photon is given by the short formula

$$\delta Z_{\gamma\gamma}^{(2)} = \Pi_{\gamma\gamma,T}^{(2)\prime}(0) - \frac{1}{4} (\delta Z_{Z\gamma}^{(1)})^2, \tag{43}$$

whereas in the mixing counterterm the vacuum expectation value correction again makes its appearance:

$$\delta Z_{Z\gamma}^{(2)} = -\frac{2}{M_Z^2} \Pi_{\gamma Z}^{(2)}(0) - \frac{1}{2} \delta Z_{ZZ}^{(1)} \delta Z_{Z\gamma}^{(1)} - \frac{1}{M_Z^2} \delta Z_{Z\gamma}^{(1)} \delta M_Z^{2(1)} - \delta Z_v^{(1)} \delta Z_{Z\gamma}^{(1)}. \tag{44}$$

In the on-shell calculation the ghost sector was also renormalized. The corresponding constants are as in [5] up to an unimportant renormalization of the ghost wave functions, the difference being dictated by simplicity. The wave function renormalization constants of the ghosts and Goldstone bosons have been left unspecified. For the ghosts, these constants cancel trivially within every closed loop. With the Goldstone bosons, the situation is more complicated, since the fact that the gauge fixing term should not be renormalized induces Goldstone wave function renormalization constants in the ghost sector. These can cancel only in gauge invariant quantities. This indeed happened for all the mass and coupling counterterms and for the complete result.

IV. $\overline{\text{MS}}$ RENORMALIZATION

In this section we describe in detail the renormalization of Δr in the $\overline{\text{MS}}$ scheme. Δr is computed through the matching procedure described before in Sec. II and defined by Eq. (4) with all parameters (masses and coupling) given also in the $\overline{\text{MS}}$ scheme. Here we choose the strategy of multiplicative renormalization. After multiplication by the on-shell wave function renormalization constants of external fermion fields, the result is expressed in terms of bare masses and bare electric charge. In order to get the $\overline{\text{MS}}$ renormalized result for G_F one needs to substitute all bare parameters in the form

$$e_0 = \mu^\varepsilon Z_e e(\mu),$$

$$(m_i^0)^2 = Z_{m_i} m_i^2(\mu), \tag{45}$$

where $e(\mu)$ and $m_i(\mu)$ are the $\overline{\rm MS}$ charge and masses, respectively, and μ is the $\overline{\rm MS}$ parameter. The $\overline{\rm MS}$ renormalization constants will be specified in the next two subsections.

Let us stress that in Eq. (45) we renormalize only the physical parameters and no renormalization of the unphysical sector (ghost sector and gauge fixing parameters) is required. The renormalization of the boson particle wave functions is also unnecessary, apart from the on-shell wave function renormalization constants in the neutral gauge sector, which are needed to define the electric charge counterterm in Sec. IV A. The $\overline{\rm MS}$ wave function counterterms cancel anyway in the final expression.

As already mentioned earlier, in order to have explicitly gauge invariant counterterms, one should take the tadpole diagrams into account properly. There are two ways to do this: either just include all possible Higgs boson tadpole diagrams in the calculation, which is done here in the $\overline{\rm MS}$ scheme or, alternatively, using the technique described in Sec. III A include the tadpoles effectively by inserting the new counterterm δZ_v. In both cases we obtained the same gauge invariant result for the counterterms.

Below we present the analytical expressions for charge and mass $\overline{\rm MS}$ renormalization constants, needed in order to obtain a finite expression for Δr in the $\overline{\rm MS}$ scheme.

A. Coupling and mass renormalization

The bare charge e_0 and the $\overline{\rm MS}$ charge e are related via

$$e_0=\mu^{\varepsilon}e\left(1+\frac{e^2(\mu)}{16\pi^2\varepsilon}Z_e^{(1,1)}+\frac{e^4(\mu)}{(16\pi^2)^2\varepsilon}Z_e^{(2,1)}+\frac{e^4(\mu)}{(16\pi^2)^2\varepsilon^2}Z_e^{(2,2)}\right), \tag{46}$$

where the constants Z's, as we shall see in the following, can depend on $\sin\theta_W$.

There are two ways to determine the $\overline{\rm MS}$ renormalization constant in this expression. One is to proceed exactly as for its on-shell counterpart in Sec. III B, i.e., from the Ward identity

$$1=Z_e\left(\sqrt{Z_{\gamma\gamma}}+\frac{1}{2}\frac{\sin\theta_W^0}{\cos\theta_W^0}\delta Z_{Z\gamma}\right). \tag{47}$$

The one- and two-loop counterterms are given by Eqs. (41) and (42), respectively, with the only difference that without renormalization of the subdivergencies the wave function renormalization constants read

$$\delta Z_{\gamma\gamma}^{(2)}=\Pi_{\gamma\gamma,T}^{(2)\prime}(0)+\delta Z_{\gamma\gamma}^{(1)}\Pi_{\gamma\gamma,T}^{(1)\prime}(0)+\delta Z_{Z\gamma}^{(1)}\Pi_{\gamma Z,T}^{(1)\prime}(0)-\frac{1}{4}(\delta Z_{Z\gamma}^{(1)}),$$

$$\delta Z_{Z\gamma}^{(2)}=-\frac{2}{M_Z^2}\left(\Pi_{\gamma Z,T}^{(2)}(0)+\frac{1}{2}\delta Z_{Z\gamma}^{(1)}\Pi_{ZZ,T}^{(1)}(0)+\frac{1}{2}\delta Z_{\gamma\gamma}^{(1)}\Pi_{\gamma Z,T}^{(1)}(0)+\frac{1}{2}\delta Z_{ZZ}^{(1)}\Pi_{\gamma Z,T}^{(1)}(0)\right)-\frac{1}{2}\delta Z_{ZZ}^{(1)}\delta Z_{Z\gamma}^{(1)}, \tag{48}$$

where this time all of the self-energies are unrenormalized. All other one-loop field renormalization constants were defined before in Sec. III B. At the end we have an expression for the on-shell charge renormalization constant expressed via the bare charge, Weinberg angle, and masses. Now, rewriting the bare quantities in terms of $\overline{\rm MS}$ ones with yet unknown coefficients in Eq. (46) and requiring that the transition between on-shell and $\overline{\rm MS}$ charges should not contain divergencies, we easily extract the $\overline{\rm MS}$ charge renormalization constants.

Alternatively, the renormalization group analysis can be applied. In order to find Z_e we differentiate Eq. (46) with respect to $\log\mu^2$ and take into account that

$$\frac{de}{d\log\mu^2}=-\frac{\varepsilon}{2}e+\beta_e, \tag{49}$$

where

$$\beta_e=\frac{e^3}{16\pi^2}b_1+\frac{e^5}{(16\pi^2)^2}b_1+\cdots \tag{50}$$

is the β function. Since $(d/d\log\mu^2)e_0=0$, the left-hand side (LHS) of Eq. (46) becomes zero after the differentiation, while the RHS relates the coefficients b_j and the unknown constants in Eq. (46):

$$Z_e^{(1,1)}=b_0,\qquad Z_e^{(2,2)}=\frac{3}{2}b_0^2,\qquad Z_e^{(2,1)}=\frac{1}{2}b_1. \tag{51}$$

The function β_e can be extracted from the existing calculation in the unbroken theory; namely, for the $SU(2)$ and $U(1)$ charges g and g', respectively, the β functions read

$$\beta_{g'}=\frac{1}{12}\frac{g'^3}{16\pi^2}+\frac{1}{4}\frac{g'^5}{(16\pi^2)^2}+\frac{3}{4}\frac{g'^3g^2}{(16\pi^2)^2},$$

$$\beta_g=-\frac{43}{12}\frac{g^3}{16\pi^2}-\frac{259}{12}\frac{g^5}{(16\pi^2)^2}+\frac{1}{4}\frac{g^3g'^2}{(16\pi^2)^2}. \tag{52}$$

The one-loop result is given in [24], while the two-loop coefficients have been evaluated in [25].

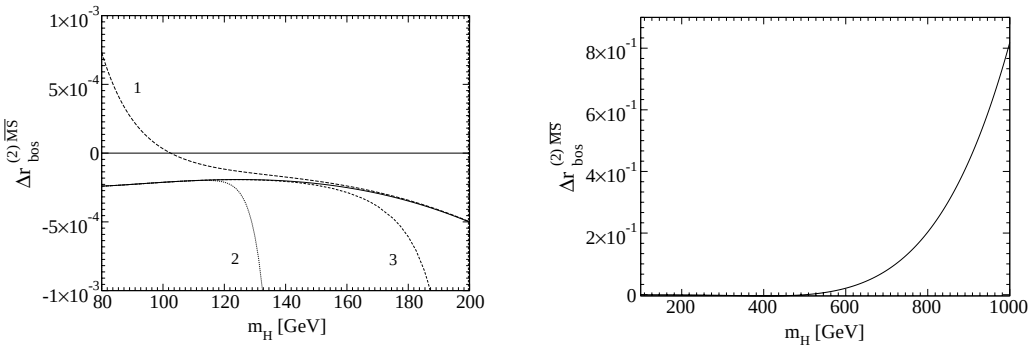

FIG. 4. The exact result (solid line) for $\Delta r^{(2)}_{\rm bos}$ in the $\overline{\rm MS}$ scheme (left and right panels) vs its (1) large Higgs boson mass expansion (long dashed line) and (2) mass difference expansion (dotted line). The short dashed line (3) represents the [3/3] Padé approximant. In the right panel the large Higgs boson mass expansion curve coincides completely with the numerical result for this range.

From the relation

$$\frac{1}{e^2}=\frac{1}{g^2}+\frac{1}{g'^2}, \tag{53}$$

it is easy to deduce that

$$\beta_e=e^3\left(\frac{\beta_g}{g^3}+\frac{\beta_{g'}}{g'^3}\right). \tag{54}$$

Using now Eqs. (52), (53), and (54) we obtain

$$\beta_e=-\frac{7}{2}\frac{e^3}{16\pi^2}+\frac{e^5}{(16\pi^2)^2}\left(-\frac{125}{6\sin^2\theta_W}+\frac{1}{2\cos^2\theta_W}\right), \tag{55}$$

and, finally, from Eq. (51) we have

$$Z_e^{(1,1)}=-\frac{7}{2},$$

$$Z_e^{(2,2)}=\frac{147}{8},$$

$$Z_e^{(2,1)}=-\frac{125}{12}\frac{1}{\sin^2\theta_W}+\frac{1}{4}\frac{1}{\cos^2\theta_W}. \tag{56}$$

The explicit calculation confirms the above result.

Similarly to the charge renormalization we write for the masses of the *Z*, *W*, and Higgs bosons

$$(m_V^0)^2=m_V^2(\mu)\left(1+\frac{g^2(\mu)}{16\pi^2\varepsilon}Z_V^{(1,1)}+\frac{g^4(\mu)}{(16\pi^2)^2\varepsilon}Z_V^{(2,1)}+\frac{g^4(\mu)}{(16\pi^2)^2\varepsilon^2}Z_V^{(2,2)}\right). \tag{57}$$

For m_Z and m_W the renormalization constants up to two loops are required while for the Higgs boson we need only the one-loop expression. The analysis, similar to that described above for the charge, has been done in detail in [19]. There the explicit expressions for $Z_V^{(1,1)}$, $Z_V^{(2,1)}$, and $Z_V^{(2,2)}$ are given.

B. $\overline{\rm MS}$ results for Δr

In Fig. 4 we plot $\Delta r^{(2)\overline{\rm MS}}_{\rm bos}$ as a function of the $\overline{\rm MS}$ Higgs boson mass in different scales. As input parameters we used the on-shell values given in Table I.

The solid curve represents the exact result. Two other curves represent expansions in different regimes: as $m_H \to m_Z$ and as $m_H \to \infty$. They cover almost the whole region of m_H under consideration. In order to extend the range of the expansion around m_Z the Padé approximant was constructed. It sufficiently improves the situation for the intermediate Higgs boson masses. Thus the expansions completely cover the region of interest. The details of the expansions are discussed more precisely in Sec. VI B.

V. TRANSITION BETWEEN THE SCHEMES

Once we have the result in the $\overline{\rm MS}$ scheme it is necessary to translate it into the on-shell parameters, which are known with high precision for the electroweak sector, contrary to the strong interacting sector of the standard model. To this end one has to consider the proper scheme independent quantity, which is

$$\frac{\alpha\pi}{2M_W^2\sin^2\theta_W}(1+\Delta r)\equiv\frac{G_F}{\sqrt{2}}. \tag{58}$$

This should be contrasted with the naive approach of taking simply Δr and substituting $\overline{\rm MS}$ parameters.

Using the methods described in Sec. IV, we obtain the following series expansions connecting on-shell and $\overline{\rm MS}$ parameters:

TABLE I. Parameter values used in the calculation [1].

α^{-1}	137.03599976(50)
M_W	80.423(39) GeV
M_Z	91.1876(21) GeV

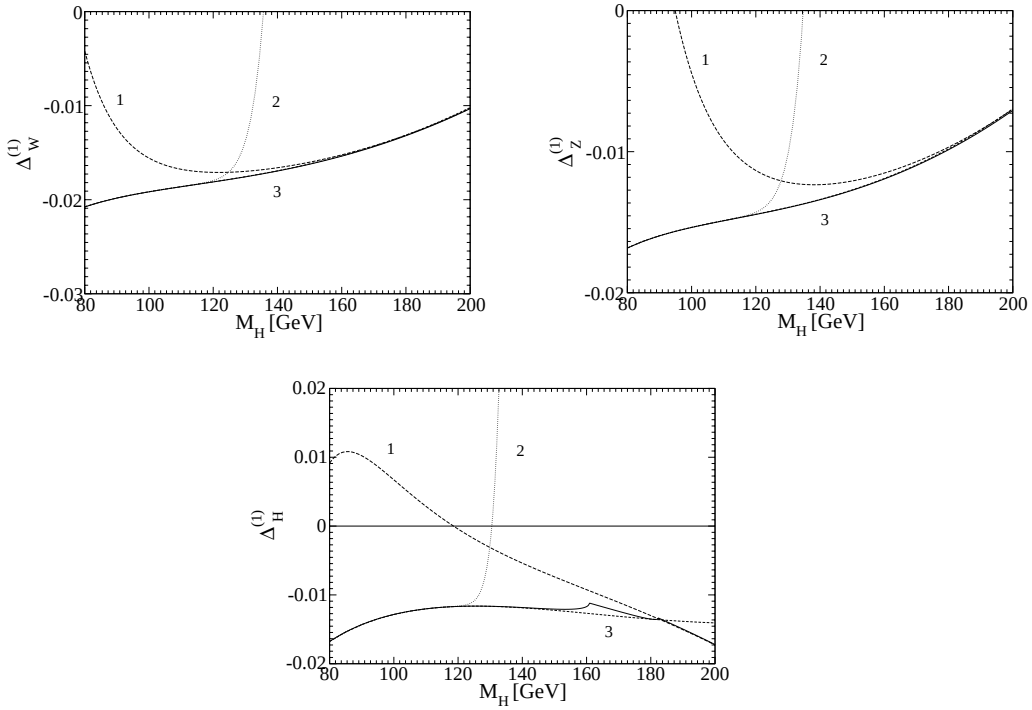

FIG. 5. One-loop corrections to the relations between the on-shell and $\overline{\mathrm{MS}}$ masses for the W, Z, and Higgs bosons $[\Delta_i^1=\alpha/(4\pi)X_1^i]$. The long dashed line (1) represents the large Higgs boson mass expansion, and the dotted line (2) represents the mass difference expansion. The short dashed line (3) gives the [4/4] Padé approximant, which coincides for this range with the exact result for the W and Z boson mass corrections.

$$\alpha_{\mathrm{OS}}=\alpha_{\overline{\mathrm{MS}}}\left[1+\frac{\alpha_{\overline{\mathrm{MS}}}}{4\pi}x^{\alpha}_{1,\overline{\mathrm{MS}}}+\left(\frac{\alpha_{\overline{\mathrm{MS}}}}{4\pi}\right)^2 x^{\alpha}_{2,\overline{\mathrm{MS}}}\right], \tag{59}$$

$$M^2_{W,\mathrm{OS}}=M^2_{W,\overline{\mathrm{MS}}}\left[1+\frac{\alpha_{\overline{\mathrm{MS}}}}{4\pi}x^{W}_{1,\overline{\mathrm{MS}}}+\left(\frac{\alpha_{\overline{\mathrm{MS}}}}{4\pi}\right)^2 x^{W}_{2,\overline{\mathrm{MS}}}\right], \tag{60}$$

$$M^2_{Z,\mathrm{OS}}=M^2_{Z,\overline{\mathrm{MS}}}\left[1+\frac{\alpha_{\overline{\mathrm{MS}}}}{4\pi}x^{Z}_{1,\overline{\mathrm{MS}}}+\left(\frac{\alpha_{\overline{\mathrm{MS}}}}{4\pi}\right)^2 x^{Z}_{2,\overline{\mathrm{MS}}}\right], \tag{61}$$

$$M^2_{H,\mathrm{OS}}=M^2_{H,\overline{\mathrm{MS}}}\left(1+\frac{\alpha_{\overline{\mathrm{MS}}}}{4\pi}x^{H}_{1,\overline{\mathrm{MS}}}\right), \tag{62}$$

where the $\overline{\mathrm{MS}}$ renormalization scale dependence has been neglected. The series for the Higgs boson mass relation is needed only to first order, since the Higgs field starts to contribute to the decay only at the one-loop level.

The above relations have to be inverted to yield the $\overline{\mathrm{MS}}$ parameters in terms of the on-shell ones. For any parameter A the relation will be written as follows:

$$A_{\overline{\mathrm{MS}}}=A_{\mathrm{OS}}\left[1+\frac{\alpha_{\mathrm{OS}}}{4\pi}X^{A}_{1,\mathrm{OS}}+\left(\frac{\alpha_{\mathrm{OS}}}{4\pi}\right)^2 X^{A}_{2,\mathrm{OS}}\right]. \tag{63}$$

The expansion coefficients are obtained by inverting the original series up to the required order. At one loop this leads trivially to

$$X^{A}_{1,\mathrm{OS}}=[-x^{A}_{1,\overline{\mathrm{MS}}}]_{M_{i,\overline{\mathrm{MS}}}\to M_{i,\mathrm{OS}}}. \tag{64}$$

The coefficients for the three bosons are depicted in Fig. 5 with parameters values as given in Table I, in a comparison of the different evaluation methods. For Higgs boson masses greater than 200 GeV the large mass expansion with six coefficients is indiscernible from the numerical result. The mass difference expansion always fails around 120 GeV. In the visible range from 80 GeV to 200 GeV, the Padé approximation based on the mass difference expansion turns out to practically coincide with the exact result for vector bosons. For the Higgs boson this cannot happen due to the occurrence of the two-particle production thresholds, and indeed there is a region between the thresholds which cannot be reproduced with either the mass difference or the large mass expansion. Obviously, if it was needed this region could be covered by threshold expansions.

The two-loop correction contains terms coming also from the one-loop terms and the proper expression reads

$$X^{A}_{2,\mathrm{OS}}=\left[-x^{A}_{2,\overline{\mathrm{MS}}}+x^{\alpha}_{1,\overline{\mathrm{MS}}}x^{A}_{1,\overline{\mathrm{MS}}}+\sum_i M^2_{i,\overline{\mathrm{MS}}}\frac{\partial x^{A}_{1,\overline{\mathrm{MS}}}}{\partial M^2_{i,\overline{\mathrm{MS}}}}x^{i}_{1,\overline{\mathrm{MS}}}\right]_{M_{i,\overline{\mathrm{MS}}}\to M_{i,\mathrm{OS}}}. \tag{65}$$

The corrections for the vector bosons are depicted similarly to the one-loop case in Fig. 6. The expansions themselves are

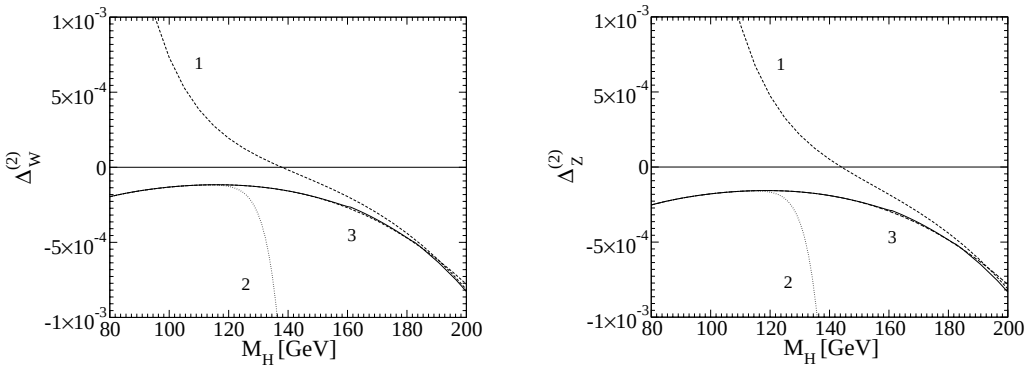

FIG. 6. Two-loop corrections to the relation between the on-shell and $\overline{\mathrm{MS}}$ masses for the W and Z bosons ($\Delta_i^2=[\alpha/(4\pi)]^2 X_2^i$). The long dashed line (1) represents the large Higgs boson mass expansion and the dotted line (2) represents the mass difference expansion. The short dashed line (3) gives the [4/4] Padé approximant.

less precise. It is, however, interesting to note that the Padé approximation together with the large mass expansion cover the whole range with high precision. Even the threshold region is reproduced with a relatively small error, although this is due to the fact that the peaks are not very pronounced.

We can now combine all the perturbative expansions and translate the $\overline{\mathrm{MS}}$ result into the on-shell one. We shall not reproduce the formula since it can easily be obtained from the previous equations. It is important, however, to note two things. First, in the expression for the two-loop Δr there are the following terms:

$$(\Delta r^{(2)})^{\mathrm{OS}}=\cdots+\frac{X^W_{2,\mathrm{OS}}}{\sin^2\theta_W}-\frac{X^Z_{2,\mathrm{OS}}}{\sin^2\theta_W}+\cdots. \qquad (66)$$

If this is combined with the fact that the results in both $\overline{\mathrm{MS}}$ and on-shell schemes behave as $1/\sin^4\theta_W$, it is obvious that one term in the W and Z boson mass difference expansion is lost. Second, the result in the $\overline{\mathrm{MS}}$ scheme behaves as M_H^4, whereas the one in the on-shell scheme behaves as M_H^2. Therefore, one term in the large Higgs boson mass expansion is also lost. As a result, if the expansions of [19] are taken, the final result can be given with five coefficients in both expansions in the large mass case. The formulas can be found in Appendix B. The mass difference expansion requires an independent calculation of the on-shell propagator diagrams and the result can be found in Appendix C. The numerical results can be found in Fig. 7. It should be stressed that it was checked that the exact analytic result without expansions obtained by the translation procedure described above and by an explicit renormalization in the on-shell scheme are the same.

It is interesting to consider the transition between the schemes performed purely numerically. In Fig. 8, the solid curve represents the one-loop correction as well as the sum of the one- and two-loop corrections. The fact that they are indiscernible on this scale is due to their relative smallness. The most reliable way of obtaining the correction (apart from the exact method) is to take the one-loop result and substitute the $\overline{\mathrm{MS}}$ parameters only in the normalization in Eq. (58), whereas the masses in $(\Delta r^{(1)}_{\mathrm{bos}})^{\overline{\mathrm{MS}}}$ should be left in the on-shell scheme. This is shown in the curve (2). If one simply takes the whole invariant, however, and substitutes all of the

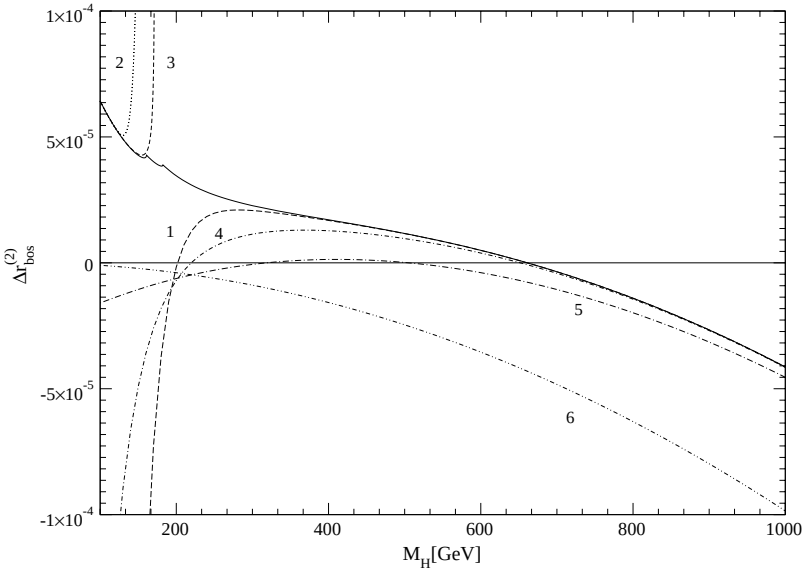

FIG. 7. On-shell $\Delta r^{(2)}_{\mathrm{bos}}$. The long dashed line (1) represents the large Higgs boson mass expansion and the dotted line (2) represents mass difference expansion. The short dashed line (3) gives the [3/3] Padé approximant. The dash-dotted lines (4) and (5) correspond to lower terms in the large Higgs boson mass expansion, whereas (6) is the leading term.

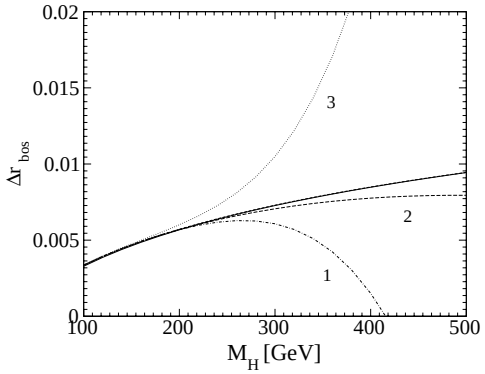

FIG. 8. Numeric translation of Δr form the $\overline{\text{MS}}$ scheme to the on-shell scheme vs the exact result (solid line).

$\overline{\text{MS}}$ parameters, then curve (1) is obtained, which diverges strongly for Higgs boson masses larger than about 250 GeV. It turns out that the sum of the one- and two-loop corrections does not reduce the scheme dependence substantially, as shown by curve (3), where the correction up to two-loop order in the $\overline{\text{MS}}$ scheme has been given for $\overline{\text{MS}}$ parameters translated from on-shell values using Eqs. (59)–(62).

VI. COMPUTATIONAL METHODS

The calculation of the bosonic corrections to the muon lifetime is a relatively complex task. The number of Feynman diagrams to be calculated is around 5000 in the R_ξ gauge. This makes it necessary to use automated software.

A. Software and checks

The first step of the calculation is the generation of diagrams. Several systems are presently available. Obviously each differs in its ease of use, speed, and design concepts.

The on-shell calculation was based on the C++ library DIAGEN [26]. It generates all diagrams together with all necessary counterterms. The main advantage of this software is the speed, since all of the diagrams were generated in a few seconds, thus making the generation phase a negligible part of the calculation.

Alternatively, for the calculation with the tadpoles the input generator DIANA [27] has been applied. We note that according to the rules given in Sec. IV no counterterm diagrams should be generated. They are all taken into account by the multiplicative renormalization.

The diagrams to be evaluated can be divided into two broad classes. First are those which can be reduced to vacuum bubbles. Here, partial integration identities [16] supplied with analytical formulas [15] can be used.

The second more complicated problem is the evaluation of the two-loop two-point functions at nonvanishing external momentum (at the values $q^2=M_Z^2$ and $q^2=M_W^2$ in our case). From the several possibilities two different algorithms have been used to deal with these diagrams.

The algorithm described in [28] has been chosen because of its simplicity. As a final result of the tensor reduction scalar two-loop propagator integrals are obtained. A high precision numerical evaluation of these is currently possible with one-dimensional integral representations [29]. To this end C++ programs were used based on the library S2LSE [30]. For large scale differences, which occur when the Higgs mass is much above the masses of the W and the Z boson, double precision turns out to be insufficient. An easy way to see it is to remark that the individual terms in the result can behave as M_H^8 whereas due to the screening theorem [31] the whole result behaves at most as M_H^2. For a Higgs boson mass of the order of 1 TeV, this means that cancellations of the order of 10^6 will have to occur. If we combine this with the fact that in double precision some of the integrals can be evaluated only to five digits, the numerical instability becomes apparent. A way out of this problem on 32-bit machines is to use software emulated quadruple precision. Of course, this signifies an important drop in effectiveness. In practice, the software runs about 20 times slower. Ten times are due to the use of software emulation for arithmetical operations and two to more integration points, which are needed for higher precision. On present gigahertz processors, the evaluation of a single point of the final result requires around 20 s and a conservative estimate of the error over the whole range of Higgs boson mass from 100 GeV to 1 TeV is four digits.

Alternatively to the numerical method, we used also a semianalytic method of expansions (see next subsection). In this case the huge cancellations mentioned above do not cause any problem.

The size of the programs written in C++ and in FORM [32] requires stringent checks. A helpful property of the bosonic corrections to the propagators is that the value of every single diagram can be obtained rather easily through low momentum or large mass expansions. In fact, for the Z boson propagators a low momentum expansion up to tenth order provided a five-digit agreement with the integral representations for each diagram independently and for the whole sum. Additionally, we also made an expansion around the point $M_H=M_Z$ (see the next subsection) and got excellent agreement between the numerical and expanded results. In the case of the W boson propagators not all of the diagrams are below threshold. It turns out that 345 contain a photon or a massless ghost line, which causes as many as around 160 of them to be either on threshold or infrared divergent. In this case the low momentum expansion either fails to converge or converges very slowly. A way out of this is given by large mass expansions. If the lines which are to be considered as heavy are chosen in a specific way, then the large mass expansion leads only to vacuum bubbles and one-loop propagator diagrams and the convergence is comparable to the case of the Z boson propagators. An example choice of the heavy lines for two different topologies is given in Fig. 9. This procedure fails only for graphs that represent pure QED corrections to a W boson line. In this case, however, the result is known analytically [33].

Another way of testing the analytical reduction and the diagram generation software is to check the Ward-Takahashi identities for the propagators. Here the following relations have been evaluated:

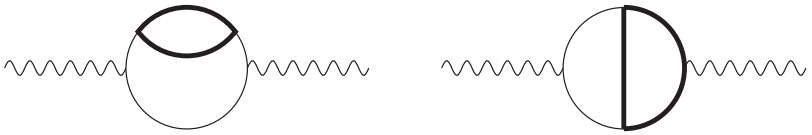

FIG. 9. A choice of formally heavy lines in the large mass expansion of two W boson propagator topologies.

$$p^2(\Pi^{(2)}_{ZZ,L}+2iM_Z\Pi^{(2)}_{ZG_Z})+M_Z^2\Pi^{(2)}_{G_ZG_Z}+p^2(\Pi^{(1)}_{ZG_Z})^2 + \Pi^{(1)}_{ZZ,L}\Pi^{(1)}_{G_ZG_Z}=0, \tag{67}$$

$$p^2(\Pi^{(2)}_{WW,L}-2M_W\Pi^{(2)}_{WG_W})+M_W^2\Pi^{(2)}_{G_WG_W}-p^2(\Pi^{(1)}_{WG_W})^2 + \Pi^{(1)}_{WW,L}\Pi^{(1)}_{G_WG_W}=0 \tag{68}$$

both for on-shell values of the momentum and in an expansion around zero up to third order. Here G_Z and G_W stand for the neutral and charged would-be Goldstone bosons, respectively, the subscript L denotes the longitudinal parts of the vector boson self-energies, and the scalar vector transitions are given by

$$\Pi^{\mu}_{VG_V}(p)=p^{\mu}\Pi_{VG_V}(p^2), \tag{69}$$

where p is the ingoing momentum of the vector boson.

The combination of the two checks described above tests the software from the diagram generation to the numerical evaluation. An additional test is of course provided by gauge invariance, and indeed the calculation was performed in the general R_ξ gauge with three independent gauge parameters. We observed explicitly the cancellation of each of them from the final result and the counterterms.

Since the bosonic corrections to the propagators in the $\overline{\rm MS}$ scheme have been evaluated within the large Higgs boson mass approach in [19] a comparison was also possible for the whole result. It turns out that the agreement is perfect for Higgs boson masses running as low as 200 GeV (see Fig. 6).

To complete the description of the computational methods, let us note that C++ and FORM were supplied with a collection of AWK and BOURNE shell scripts managed by several MAKEFILES. The system prepared in this way runs completely automatically from the beginning with diagram generation up to the numerical evaluation with plots. Actually, the specificity of the problem allowed reduction of the evaluation time of the whole problem down to only one hour and a half, which is rather short for multiloop calculations.

B. Expansions

Here we give more details on how the expansions are performed in two different regimes that we considered: in the mass difference $h_Z=(M_H^2-M_Z^2)/M_Z^2$ and in the mass ratio $z_H=M_Z^2/M_H^2$.

The expansion in the mass difference $M_H^2-M_Z^2$ is especially simple. It is just a Taylor expansion of all Higgs propagators and Higgs boson masses in the vertices around M_Z. No additional subgraphs are necessary in this case. The expansion in the heavy Higgs boson limit is somewhat more involved. It is given by the rules of asymptotic expansions [13].

In addition, in the presence of both M_Z and M_W we expand in the difference of these masses as well. Indeed,

$$\frac{M_Z^2-M_W^2}{M_Z^2}=\sin^2\theta_W\approx 0.23 \tag{70}$$

is a rather small parameter and the convergence of this series is quite fast. This trick was used previously in [19]. The advantage of this approach is that in the case of on-shell Green's functions all integrals have only one scale. This allows one to use the FORM package ONSHELL2 [34] to evaluate these integrals analytically.

We should also note that to extend the range of the h_Z expansion we apply the Padé approximation. Throughout this paper we use a [3/3] Padé approximant for Δr and [4/4] for the scheme transition formulas. The Padé approximation for the z_H series does not work well since this series is nonalternating.

VII. CONCLUSIONS

A recent calculation of the two-loop bosonic corrections to Δr performed by two independent groups has been described in detail, from the matching to the Fermi theory to the renormalization and the explicit results in the on-shell and $\overline{\rm MS}$ schemes. The framework for the evaluation of the Fermi constant G_F based on the low energy factorization theorem has been constructed. It allows one to compute G_F as a Wilson coefficient in a simple manner. This approach is general and is also applicable to other low energy quantities.

A comparison of different expansions and numerical methods has been given. It has been proven that in a wide range of Higgs boson masses expansions provide as much precision as needed and cover the whole region of interest. The only problematic region, however, is connected to the thresholds for W and Z boson pair production. If the Higgs boson was indeed found in this range, then a precise result could also be obtained with expansions, but this time of the threshold type. The coincidence of the numerical and analytical results serves as a strong check on the calculation.

The accuracy of the numerical transformation between $\overline{\rm MS}$ and on-shell schemes has been tested. It is shown that for Higgs boson masses larger than $\sim$250 GeV the two-loop correction does not reduce the scheme dependence, which can be explained by huge cancellations of large terms during the transition procedure.

ACKNOWLEDGMENTS

The authors would like to thank K. Chetyrkin for fruitful discussions. A.O. and O.V. thank M. Tentyukov for his help with DIANA. M.A. would like to thank the Marie Curie Programme of the European Commission for a stipend. M.C. would like to thank the Alexander von Humboldt foundation for financial support. This work was supported in part by the European Community's Human Potential Program under Contract HPRN-CT-2000-00149 Physics at Colliders, by the KBN Grants 5P03B09320 and 2P03B05418, by DFG-Forschergruppe ''Quantenfeldtheorie, Computeralgebra und Monte-Carlo-Simulation'' (Contract FOR 264/2-1), and by BMBF under Grant No. 05HT9VKB0.

APPENDIX A: $U(1)$ WARD IDENTITY AND THE RENORMALIZATION OF CHARGE

In this appendix we present a derivation of the relation between the charge renormalization constant and different wave function renormalization constants valid to all orders of perturbation theory. The derivation is based on the use of the $U(1)$ Ward-Takahashi identity for the weak hypercharge gauge group. To begin with, let us take the bare $U(1)$ gauge boson field B_μ^0 and rewrite it in terms of mass eigenstates:

$$B_\mu^0 = c_W^0 A_\mu^0 + s_W^0 Z_\mu^0 . \tag{A1}$$

Here $c_W^0 = \cos\theta_W^0$ and $s_W^0 = \sin\theta_W^0$ are the bare values of the cosine and sine of the Weinberg angle.

In the next step we express our bare gauge boson fields through the renormalized ones:

$$(Z_2^B)^{1/2}\{c_W A_\mu + s_W Z_\mu\} = c_W^0\left\{\frac{1}{2} Z_{\gamma Z} Z_\mu + (Z_{\gamma\gamma})^{1/2} A_\mu\right\} + s_W^0\left\{(Z_{ZZ})^{1/2} Z_\mu + \frac{1}{2} Z_{Z\gamma} A_\mu\right\}. \tag{A2}$$

Now taking the coefficient in front of A_μ in the equation above we have

$$(Z_2^B)^{1/2} c_W = c_W^0 (Z_{\gamma\gamma})^{1/2} + \frac{1}{2} s_W^0 Z_{Z\gamma} . \tag{A3}$$

To complete the derivation we need to relate the Z_2^B renormalization constant to the charge renormalization constant. The electric charge is related to the weak hypercharge via the following equation:

$$e^0 = g_1^0 c_W^0 = (Z_2^B)^{-1/2} g_1 c_W^0 = Z_e e = Z_e g_1 c_W , \tag{A4}$$

where we have made use of the $U(1)$ Ward-Takahashi identity $Z_{g_1} = (Z_2^B)^{-1/2}$. Now we can easily deduce that

$$Z_e = (Z_2^B)^{-1/2} \frac{c_W^0}{c_W} . \tag{A5}$$

Substituting this relation into Eq. (A3) we have

$$1 = Z_e\left\{(Z_{\gamma\gamma})^{1/2} + \frac{s_W^0}{c_W^0}\frac{1}{2} Z_{Z\gamma}\right\}. \tag{A6}$$

Using this final relation one can considerably simplify the calculation of the on-shell charge renormalization constant and avoid dealing with infrared rearrangement while computing the three-point Green's function.

APPENDIX B: LARGE HIGGS BOSON MASS EXPANSION OF $\Delta r_{\rm bos}^{(2)}$ IN THE ON-SHELL SCHEME

In this appendix, the on-shell renormalized $\Delta r_{\rm bos}^{(2)}$ is given in a twofold expansion, in the large Higgs boson mass and in the mass difference between the W and Z bosons. The number of terms is consistent with the result [19] as explained in Sec. V. The leading behavior both in the Higgs boson mass and in the sine of the Weinberg angle has been factorized out:

$$(\Delta r_{\rm bos}^{(2)})^{\rm OS} = \left(\frac{\alpha}{4\pi \sin^2\theta_W}\right)^2 \frac{M_H^2}{M_Z^2} \sum_{n=0}^{4} \sin^{2n}\theta_W R_n^{\rm OS} . \tag{B1}$$

The occurring transcendental numbers are

$$S_1 = \frac{\pi}{\sqrt{3}},$$

$$S_2 = \frac{4}{9}\frac{{\rm Cl}_2(\pi/3)}{\sqrt{3}} \simeq 0.260434137632162098955729143208030 8\ldots , \tag{B2}$$

while $z_H = M_Z^2/M_H^2$. Note that the leading term in the Higgs boson mass can be resummed in $\sin^2\theta_W$ to give the behavior

$$\Delta r_{\rm Higgs}^{(2)} = \left(\frac{\alpha}{4\pi \sin^2\theta_W}\right)^2 \frac{M_H^2}{8M_W^2}\left[9\sqrt{3}{\rm Cl}_2\left(\frac{\pi}{3}\right) + \frac{49}{72} - \frac{11\pi\sqrt{3}}{4} - \frac{25\pi^2}{108}\right]. \tag{B3}$$

The expansion coefficients read

$$R_0^{\mathrm{OS}}=\left[-\frac{33}{32}S_1-\frac{25}{144}\zeta_2+\frac{49}{576}+\frac{243}{32}S_2\right]+z_H\left[-\frac{303659}{384}S_1-\frac{1515}{16}\zeta_3-\frac{125}{4}\ln(z_H)S_1+\frac{41}{288}\ln(z_H)^2+\frac{17305}{576}\zeta_2\right.$$
$$\left.+\frac{98125}{1728}\ln(z_H)+\frac{4131}{32}S_1S_2+\frac{1089}{8}S_1^2+\frac{7069829}{20736}+\frac{259443}{128}S_2+66\ln(3)\zeta_2\right]+z_H^2\left[-\frac{75341}{960}S_1-\frac{41441}{1440}\zeta_2\right.$$
$$\left.-\frac{83}{48}\ln(z_H)^2+\frac{5940941}{86400}+\frac{42481}{320}\ln(z_H)+\frac{72171}{320}S_2-95\ln(z_H)S_1\right]+z_H^3\left[-\frac{1519543}{3200}S_1-\frac{29439}{80}\ln(z_H)S_1-\frac{4031}{30}\zeta_2\right.$$
$$\left.-\frac{70567}{2880}\ln(z_H)^2+\frac{6319637}{17280}\ln(z_H)+\frac{599726311}{1296000}+\frac{95067}{160}S_2\right]+z_H^4\left[-\frac{34374449}{16800}S_1-\frac{7468}{5}\ln(z_H)S_1-\frac{1837867}{3360}\zeta_2\right.$$
$$\left.-\frac{92423}{720}\ln(z_H)^2+\frac{11836033}{10800}\ln(z_H)+\frac{3853287}{2240}S_2+\frac{47950477091}{25401600}\right],$$

$$R_1^{\mathrm{OS}}=\left[-\frac{33}{32}S_1-\frac{25}{144}\zeta_2+\frac{49}{576}+\frac{243}{32}S_2\right]+z_H\left[-\frac{772245}{128}S_2-\frac{4850423}{2304}-\frac{8349}{16}S_1^2-\frac{14733}{32}S_1S_2-\frac{44117}{192}\zeta_2\right.$$
$$\left.-\frac{24641}{192}\ln(z_H)+\frac{115}{288}\ln(z_H)^2+\frac{6541}{96}\ln(z_H)S_1+\frac{5653}{16}\zeta_3+\frac{3844355}{1152}S_1-264\ln(3)\zeta_2-66\ln(3)S_1+96\ln(2)\zeta_2\right]$$
$$+z_H^2\left[-\frac{373487}{960}\ln(z_H)-\frac{7519453}{28800}-\frac{40167}{160}S_2+\frac{203}{72}\ln(z_H)^2+\frac{47807}{720}\zeta_2+\frac{248651}{1440}S_1+\frac{11653}{48}\ln(z_H)S_1\right]$$
$$+z_H^3\left[-\frac{5103328117}{2592000}-\frac{108967649}{86400}\ln(z_H)-\frac{22023}{80}S_2+\frac{189529}{2880}\ln(z_H)^2+\frac{3561}{10}\zeta_2+\frac{168033}{160}\ln(z_H)S_1\right.$$
$$\left.+\frac{13792549}{9600}S_1\right]+z_H^4\left[-\frac{11560206263}{1296000}-\frac{1265074333}{302400}\ln(z_H)+\frac{122819}{288}\ln(z_H)^2+\frac{44091}{56}S_2+\frac{4466227}{2520}\zeta_2\right.$$
$$\left.+\frac{58457}{12}\ln(z_H)S_1+\frac{72817723}{10080}S_1\right],$$

$$R_2^{\mathrm{OS}}=\left[-\frac{33}{32}S_1-\frac{25}{144}\zeta_2+\frac{49}{576}+\frac{243}{32}S_2\right]+z_H\left[-\frac{1857047}{384}S_1-\frac{17687}{48}\zeta_3-\frac{635}{32}\ln(z_H)S_1+\frac{115}{288}\ln(z_H)^2+\frac{21407}{576}\ln(z_H)\right.$$
$$\left.+\frac{11109}{32}S_1S_2+\frac{256511}{576}\zeta_2+\frac{4719}{8}S_1^2+\frac{535053}{128}S_2+\frac{94100843}{20736}-192\ln(2)\zeta_2+242\ln(3)S_1+288\ln(3)\zeta_2\right]$$
$$+z_H^2\left[-\frac{172439}{960}S_1-\frac{2539}{16}\ln(z_H)S_1-\frac{33067}{720}\zeta_2+\frac{11}{12}\ln(z_H)^2+\frac{32847}{160}S_2+\frac{2467333}{8640}\ln(z_H)+\frac{165415279}{518400}\right]$$
$$+z_H^3\left[-\frac{1135551}{640}S_1-\frac{8525}{8}\ln(z_H)S_1-\frac{23417}{80}\zeta_2-\frac{12427}{576}\ln(z_H)^2+\frac{19761}{40}S_2+\frac{136065731}{86400}\ln(z_H)+\frac{590467441}{216000}\right]$$
$$+z_H^4\left[-\frac{189343717}{16800}S_1-\frac{32914}{5}\ln(z_H)S_1-\frac{5087309}{2520}\zeta_2-\frac{116609}{360}\ln(z_H)^2-\frac{675}{112}S_2+\frac{90743033}{12096}\ln(z_H)\right.$$
$$\left.+\frac{139434492997}{9072000}\right],$$

$$R_3^{\mathrm{OS}}=\left[-\frac{33}{32}S_1-\frac{25}{144}\zeta_2+\frac{49}{576}+\frac{243}{32}S_2\right]+z_H\left[-\frac{29707045}{10368}-\frac{77817}{64}S_2-\frac{366221}{864}\zeta_2-\frac{5071}{24}S_1^2-\frac{589}{3}\ln(3)S_1\right.$$
$$\left.-\frac{664}{9}\ln(3)\zeta_2-\frac{709}{16}S_1S_2-\frac{5257}{1728}\ln(z_H)+\frac{115}{288}\ln(z_H)^2+\frac{1739}{864}\ln(z_H)S_1+\frac{10357}{72}\zeta_3+\frac{1769833}{648}S_1\right]$$
$$+z_H^2\left[-\frac{46220713}{259200}-\frac{36923}{960}\ln(z_H)+\frac{11}{12}\ln(z_H)^2+\frac{2221}{108}\ln(z_H)S_1+\frac{31091}{1440}\zeta_2+\frac{1428847}{25920}S_1+\frac{41379}{320}S_2\right]$$

$$+z_H^3\left[-\frac{2086198469}{1036800}-\frac{35333761}{43200}\ln(z_H)+\frac{12311}{2880}\ln(z_H)^2+\frac{109387}{960}\zeta_2+\frac{121301}{640}S_2+\frac{110077}{240}\ln(z_H)S_1\right.$$
$$\left.+\frac{45009703}{43200}S_1\right]+z_H^4\left[-\frac{658300265597}{42336000}-\frac{227753417}{33600}\ln(z_H)+\frac{9103}{80}\ln(z_H)^2+\frac{623873}{840}S_2+\frac{99685}{84}\zeta_2\right.$$
$$\left.+\frac{2489969}{540}\ln(z_H)S_1+\frac{4336498723}{453600}S_1\right],$$

$$R_4^{\rm OS}=\left[-\frac{33}{32}S_1-\frac{25}{144}\zeta_2+\frac{49}{576}+\frac{243}{32}S_2\right]+z_H\left[-\frac{52145731}{77760}S_1-\frac{1589}{32}S_1S_2-\frac{7069}{144}S_1^2-\frac{5563}{144}\zeta_3-\frac{8165}{2592}\ln(z_H)S_1\right.$$
$$\left.+\frac{115}{288}\ln(z_H)^2+\frac{49141}{8640}\ln(z_H)+\frac{350}{9}\ln(3)S_1+\frac{404}{9}\ln(3)\zeta_2+\frac{689639}{1920}S_2+\frac{1039343}{2880}\zeta_2+\frac{6966953}{11520}\right]+z_H^2\left[-\frac{4768757}{103680}\right.$$
$$\left.-\frac{16457}{1296}\ln(z_H)S_1-\frac{32123}{4860}S_1+\frac{11}{12}\ln(z_H)^2+\frac{3463}{270}\zeta_2+\frac{197509}{8640}\ln(z_H)+\frac{31313}{240}S_2\right]+z_H^3\left[-\frac{20245553}{64800}S_1\right.$$
$$\left.-\frac{141593}{1440}\ln(z_H)S_1+\frac{12311}{2880}\ln(z_H)^2+\frac{25951}{720}\zeta_2+\frac{5251313}{28800}\ln(z_H)+\frac{109751}{480}S_2+\frac{2537501}{5400}\right]+z_H^4\left[-\frac{633111511}{136080}S_1\right.$$
$$\left.-\frac{141862}{81}\ln(z_H)S_1-\frac{355907}{5040}\zeta_2+\frac{12071}{720}\ln(z_H)^2+\frac{2867831}{3360}S_2+\frac{118206539}{37800}\ln(z_H)+\frac{1002609122909}{127008000}\right].$$

APPENDIX C: MASS DIFFERENCE EXPANSION OF $\Delta r_{\rm bos}^{(2)}$ IN THE ON-SHELL SCHEME

The correction $\Delta r_{\rm bos}^{(2)}$ in the on-shell scheme for Higgs boson masses in the vicinity of the Z boson mass is correctly described by an expansion in the mass difference between the Higgs boson and the Z boson and in the mass difference between the W and Z bosons. The series below contains five terms in both variables:

$$(\Delta r_{\rm bos}^{(2)})^{\rm OS}=\left(\frac{\alpha}{4\pi\sin^2\theta_W}\right)^2\sum_{n=0}^{4}\sin^{2n}\theta_W R_n^{\rm OS}. \tag{C1}$$

The transcendental numbers are the same as in the previous section. The lack of logarithms of mass ratios follows from the fact that a Taylor series in the mass difference does not lead to any infrared problems. The variable h_Z denotes $(M_H^2-M_Z^2)/M_Z^2$:

$$R_0^{\rm OS}=\left[+\frac{20659}{48}+62\zeta_2\ln(3)+\frac{7151}{144}\zeta_2-\frac{403}{6}\zeta_3+\frac{75}{4}S_1S_2+6S_1\ln(3)-\frac{10375}{12}S_1+\frac{2909}{18}S_1^2+\frac{59629}{32}S_2\right]+h_Z\left[+\frac{2783}{288}\right.$$
$$\left.+\frac{44}{9}\zeta_2\ln(3)-\frac{2489}{144}\zeta_2-\frac{371}{18}\zeta_3+\frac{305}{4}S_1S_2-\frac{4}{3}S_1\ln(3)-\frac{959}{18}S_1+\frac{3271}{216}S_1^2+\frac{5201}{32}S_2\right]+h_Z^2\left[-\frac{43603}{1728}-\frac{4}{3}\zeta_2\ln(3)\right.$$
$$\left.-\frac{4477}{864}\zeta_2+\frac{5}{16}\zeta_3+\frac{99}{32}S_1S_2+\frac{5}{3}S_1\ln(3)+\frac{8587}{216}S_1-\frac{823}{81}S_1^2-\frac{3595}{192}S_2\right]+h_Z^3\left[+\frac{194641}{15552}+\frac{4}{9}\zeta_2\ln(3)-\frac{16531}{1296}\zeta_2-\frac{35}{36}\zeta_3\right.$$
$$\left.+\frac{23}{8}S_1S_2-\frac{1}{3}S_1\ln(3)-\frac{3491}{720}S_1+\frac{5615}{972}S_1^2-\frac{12373}{864}S_2\right]+h_Z^4\left[-\frac{88369}{17280}+\frac{151487}{23328}\zeta_2-\frac{1}{12}\zeta_3+\frac{3}{8}S_1S_2+\frac{31}{162}S_1\ln(3)\right.$$
$$\left.+\frac{113201}{12960}S_1-\frac{33611}{5832}S_1^2-\frac{1937}{288}S_2\right],$$

$$R_1^{\rm OS}=\left[-\frac{166967}{72}+96\zeta_2\ln(2)-\frac{2260}{9}\zeta_2\ln(3)-\frac{9565}{36}\zeta_2+\frac{4789}{18}\zeta_3-\frac{445}{4}S_1S_2-\frac{238}{3}S_1\ln(3)+\frac{31450}{9}S_1-\frac{62045}{108}S_1^2\right.$$
$$\left.-\frac{45355}{8}S_2\right]+h_Z\left[-\frac{24917}{864}-\frac{68}{9}\zeta_2\ln(3)-\frac{409}{432}\zeta_2+\frac{707}{18}\zeta_3-\frac{605}{4}S_1S_2+\frac{14}{3}S_1\ln(3)+\frac{24007}{216}S_1-\frac{8869}{324}S_1^2-\frac{17111}{96}S_2\right]$$
$$+h_Z^2\left[+\frac{247739}{5184}+\frac{4}{3}\zeta_2\ln(3)-\frac{52787}{2592}\zeta_2-\frac{65}{16}\zeta_3+\frac{441}{32}S_1S_2-S_1\ln(3)-\frac{106343}{4320}S_1+\frac{15737}{1296}S_1^2-\frac{31285}{576}S_2\right]$$

$$+h_Z^3\left[-\frac{1085639}{155520}+\frac{4}{9}\zeta_2\ln(3)+\frac{137425}{11664}\zeta_2-\frac{37}{72}\zeta_3+\frac{13}{16}S_1S_2+\frac{35}{81}S_1\ln(3)-\frac{92377}{77760}S_1-\frac{29293}{5832}S_1^2+\frac{21419}{864}S_2\right]$$

$$+h_Z^4\left[+\frac{4592603}{777600}-\frac{532225}{23328}\zeta_2-\frac{1}{12}\zeta_3+\frac{3}{8}S_1S_2+\frac{7}{54}S_1\ln(3)+\frac{10434679}{816480}S_1+\frac{80429}{34992}S_1^2-\frac{3611}{1728}S_2\right],$$

$$R_2^{\rm OS}=\left[+\frac{5908523}{1296}-192\zeta_2\ln(2)+\frac{2536}{9}\zeta_2\ln(3)+\frac{21139}{48}\zeta_2-\frac{2897}{9}\zeta_3+\frac{317}{2}S_1S_2+245S_1\ln(3)-\frac{1559051}{324}S_1+\frac{5426}{9}S_1^2\right.$$

$$\left.+\frac{1132651}{288}S_2\right]+h_Z\left[+\frac{746443}{15552}-\frac{32}{9}\zeta_2\ln(3)-\frac{10121}{324}\zeta_2+\frac{79}{9}\zeta_3-\frac{55}{2}S_1S_2+\frac{1}{3}S_1\ln(3)-\frac{6461}{1440}S_1+\frac{19085}{1944}S_1^2\right.$$

$$\left.-\frac{20417}{432}S_2\right]+h_Z^2\left[+\frac{214469}{155520}+\frac{8}{3}\zeta_2\ln(3)+\frac{43439}{2592}\zeta_2-\frac{173}{48}\zeta_3+\frac{231}{32}S_1S_2-\frac{41}{27}S_1\ln(3)-\frac{293137}{77760}S_1-\frac{605}{162}S_1^2\right.$$

$$\left.-\frac{70549}{1728}S_2\right]+h_Z^3\left[-\frac{3867907}{1166400}-\frac{13853}{486}\zeta_2+\frac{9}{8}\zeta_3-\frac{81}{16}S_1S_2+\frac{83}{81}S_1\ln(3)+\frac{8558191}{489888}S_1+\frac{311}{729}S_1^2+\frac{162193}{2592}S_2\right]$$

$$+h_Z^4\left[+\frac{7035509}{979776}-\frac{16024969}{559872}\zeta_2+\frac{1}{12}\zeta_3-\frac{3}{8}S_1S_2+\frac{1}{27}S_1\ln(3)+\frac{21579127}{699840}S_1-\frac{58837}{13122}S_1^2-\frac{41531}{7776}S_2\right],$$

$$R_3^{\rm OS}=\left[-\frac{5582263}{1944}-\frac{704}{9}\zeta_2\ln(3)-\frac{281321}{648}\zeta_2+\frac{5581}{36}\zeta_3-\frac{637}{8}S_1S_2-\frac{586}{3}S_1\ln(3)+\frac{109883}{40}S_1-\frac{17078}{81}S_1^2-\frac{521903}{432}S_2\right]$$

$$+h_Z\left[+\frac{437711}{25920}-\frac{8}{9}\zeta_2\ln(3)+\frac{139991}{5832}\zeta_2+\frac{343}{36}\zeta_3-\frac{319}{8}S_1S_2-\frac{181}{81}S_1\ln(3)-\frac{536677}{38880}S_1-\frac{6535}{5832}S_1^2-\frac{659}{12}S_2\right]$$

$$+h_Z^2\left[-\frac{15188507}{777600}+\frac{8}{3}\zeta_2\ln(3)-\frac{355457}{46656}\zeta_2-\frac{29}{24}\zeta_3-\frac{57}{16}S_1S_2-\frac{125}{81}S_1\ln(3)+\frac{27541403}{1088640}S_1-\frac{45707}{8748}S_1^2+\frac{69397}{3456}S_2\right]$$

$$+h_Z^3\left[-\frac{25783}{2449440}-\frac{8}{9}\zeta_2\ln(3)-\frac{926609}{17496}\zeta_2+\frac{163}{36}\zeta_3-\frac{139}{8}S_1S_2+\frac{299}{243}S_1\ln(3)+\frac{4479889}{136080}S_1-\frac{11707}{13122}S_1^2+\frac{1926995}{15552}S_2\right]$$

$$+h_Z^4\left[+\frac{9642347291}{342921600}-\frac{559304957}{5038848}\zeta_2+\frac{1}{2}\zeta_3-\frac{9}{4}S_1S_2-\frac{401}{2187}S_1\ln(3)+\frac{386672993}{4199040}S_1-\frac{646097}{157464}S_1^2+\frac{27433}{3888}S_2\right],$$

$$R_4^{\rm OS}=\left[+\frac{23299549}{38880}+\frac{376}{9}\zeta_2\ln(3)+\frac{4413259}{11664}\zeta_2-\frac{343}{18}\zeta_3-\frac{509}{4}S_1S_2+\frac{6223}{162}S_1\ln(3)-\frac{25615403}{38880}S_1-\frac{12640}{243}S_1^2\right.$$

$$\left.+\frac{1314829}{4320}S_2\right]+h_Z\left[-\frac{50017}{5400}+\frac{4}{9}\zeta_2\ln(3)+\frac{1726547}{58320}\zeta_2+\frac{91}{9}\zeta_3-47S_1S_2-\frac{73}{18}S_1\ln(3)-\frac{2747231}{816480}S_1-\frac{114823}{17496}S_1^2\right.$$

$$\left.+\frac{31919}{1440}S_2\right]+h_Z^2\left[-\frac{637699471}{16329600}+\frac{4}{3}\zeta_2\ln(3)-\frac{3912127}{174960}\zeta_2+\frac{239}{48}\zeta_3-\frac{861}{32}S_1S_2-\frac{293}{162}S_1\ln(3)+\frac{2714011}{68040}S_1\right.$$

$$\left.-\frac{530147}{104976}S_1^2+\frac{284597}{2592}S_2\right]+h_Z^3\left[+\frac{308051815}{13716864}-\frac{20}{9}\zeta_2\ln(3)-\frac{3545221483}{25194240}\zeta_2+\frac{91}{9}\zeta_3-38S_1S_2+\frac{3365}{4374}S_1\ln(3)\right.$$

$$\left.+\frac{1296774019}{14696640}S_1+\frac{40363}{78732}S_1^2+\frac{16604743}{77760}S_2\right]+h_Z^4\left[+\frac{368208335437}{4115059200}-\frac{8071459297}{26873856}\zeta_2+\frac{5}{4}\zeta_3-\frac{45}{8}S_1S_2\right.$$

$$\left.-\frac{2627}{4374}S_1\ln(3)+\frac{6605645449}{29393280}S_1-\frac{2503867}{944784}S_1^2+\frac{3650279}{116640}S_2\right].$$

APPENDIX D: LARGE HIGGS BOSON MASS EXPANSION OF $\Delta r_{\rm bos}^{(2)}$ IN THE $\overline{\rm MS}$ SCHEME

In this appendix, $\Delta r_{\rm bos}^{(2)}$ renormalized in the $\overline{\rm MS}$ scheme is presented as a twofold expansion in the large Higgs boson mass and in the mass difference between the W and the Z bosons. The expansion is parametrized as follows:

$$(\Delta r^{(2)}_{\rm bos})^{\overline{\rm MS}} = \left(\frac{\alpha}{4\pi \sin^2\theta_W}\right)^2 \frac{m_H^4}{m_Z^4} \sum_{n=0}^{5} \sin^{2n}\theta_W R_n^{\overline{\rm MS}}. \tag{D1}$$

The parameters, i.e., masses, and the coupling constant are in the $\overline{\rm MS}$ scheme. Apart from the numbers Eq. (B2), it is assumed that $\ln(m^2_{Z,H}) = \ln(m^2_{Z,H}/\mu^2)$, μ being the $\overline{\rm MS}$ renormalization scale:

$$\begin{aligned}
R_0^{\overline{\rm MS}} = {} & \left[-\frac{243}{32}S_2 - \frac{27}{8}\ln(m_H^2) + \frac{1}{4}\zeta_2 + \frac{27}{32}\ln(m_H^2)^2 + \frac{457}{128}\right] + z_H\left[-\frac{243}{32}S_2 - \frac{237}{32} - \frac{45}{16}\zeta_2 - \frac{9}{4}\ln(m_H^2)^2 - \frac{9}{8}\ln(m_Z^2)\ln(m_H^2)\right. \\
& \left. + \frac{21}{16}\ln(m_Z^2) + \frac{123}{16}\ln(m_H^2)\right] + z_H^2\left[-\frac{567}{32}S_2 - \frac{53}{3}\ln(m_H^2) - \frac{805}{48}\ln(m_Z^2) + \frac{195}{32}\ln(m_Z^2)^2 + \frac{131}{16}\ln(m_H^2)^2 + \frac{113}{8}\zeta_2 + \frac{34243}{1152}\right. \\
& \left. - 2\ln(m_Z^2)\ln(m_H^2)\right] + z_H^3\left[-\frac{55831}{576} - \frac{2881}{48}\ln(m_H^2) - \frac{649}{16}\ln(m_Z^2)^2 - \frac{15}{16}\ln(m_H^2)^2 + \frac{3}{16}\zeta_2 + \frac{37}{4}\ln(m_Z^2)\ln(m_H^2)\right. \\
& \left. + \frac{4697}{24}\ln(m_Z^2) + \frac{14499}{32}S_2\right] + z_H^4\left[-\frac{7783}{96}\ln(m_H^2) - \frac{731}{32}\ln(m_Z^2)^2 - \frac{307}{16}\zeta_2 - \frac{287}{32}\ln(m_H^2)^2 + \frac{151399}{14400} + \frac{509}{16}\ln(m_Z^2)\ln(m_H^2)\right. \\
& \left. + \frac{5215}{96}\ln(m_Z^2) + 243S_2\right] + z_H^5\left[-\frac{68129}{672}\ln(m_H^2) - \frac{931}{16}\zeta_2 - \frac{779}{16}\ln(m_Z^2)^2 - \frac{453}{16}\ln(m_H^2)^2 + \frac{44394899}{1411200} + \frac{63761}{672}\ln(m_Z^2)\right. \\
& \left. + \frac{11745}{32}S_2 + 77\ln(m_Z^2)\ln(m_H^2)\right],
\end{aligned}$$

$$\begin{aligned}
R_1^{\overline{\rm MS}} = {} & \left[-\frac{243}{16}S_2 - \frac{27}{4}\ln(m_H^2) + \frac{1}{2}\zeta_2 + \frac{27}{16}\ln(m_H^2)^2 + \frac{457}{64}\right] + z_H\left[-\frac{181}{16} - \frac{243}{32}S_2 - \frac{63}{16}\zeta_2 - \frac{45}{16}\ln(m_H^2)^2 - \frac{27}{16}\ln(m_Z^2)\ln(m_H^2)\right. \\
& \left. + \frac{63}{32}\ln(m_Z^2) + \frac{177}{16}\ln(m_H^2)\right] + z_H^2\left[-\frac{1269}{32}S_2 - \frac{1073}{96}\ln(m_Z^2) - \frac{113}{48}\ln(m_H^2) - \frac{5}{8}\ln(m_Z^2)\ln(m_H^2) + \frac{19}{32}\ln(m_Z^2)^2 + \frac{43}{16}\zeta_2\right. \\
& \left. + \frac{91}{32}\ln(m_H^2)^2 + \frac{20845}{576}\right] + z_H^3\left[-\frac{4833}{8}S_2 - \frac{10445}{96}\ln(m_Z^2) - \frac{54875}{1152} - \frac{167}{32}\ln(m_H^2)^2 + \frac{1}{4}\ln(m_Z^2)\ln(m_H^2) + \frac{847}{32}\ln(m_Z^2)^2\right. \\
& \left. + \frac{3835}{96}\ln(m_H^2) - 12\zeta_2\right] + z_H^4\left[-\frac{16659}{32}S_2 - \frac{3929}{40}\ln(m_Z^2) - \frac{6123}{160} + \frac{297}{32}\ln(m_H^2)^2 + \frac{329}{16}\zeta_2 + \frac{1239}{32}\ln(m_Z^2)^2 + \frac{5499}{40}\ln(m_H^2)\right. \\
& \left. - 48\ln(m_Z^2)\ln(m_H^2)\right] + z_H^5\left[-\frac{9045}{8}S_2 - \frac{168283}{840}\ln(m_Z^2) - \frac{1579}{8}\ln(m_Z^2)\ln(m_H^2) - \frac{84807787}{705600} + \frac{2171}{32}\ln(m_H^2)^2\right. \\
& \left. + \frac{4145}{32}\ln(m_Z^2)^2 + \frac{1119}{8}\zeta_2 + \frac{200833}{840}\ln(m_H^2)\right],
\end{aligned}$$

$$\begin{aligned}
R_2^{\overline{\rm MS}} = {} & \left[-\frac{729}{32}S_2 - \frac{81}{8}\ln(m_H^2) + \frac{3}{4}\zeta_2 + \frac{81}{32}\ln(m_H^2)^2 + \frac{1371}{128}\right] + z_H\left[-\frac{473}{32} - \frac{243}{32}S_2 - \frac{81}{16}\zeta_2 - \frac{27}{8}\ln(m_H^2)^2 - \frac{9}{4}\ln(m_Z^2)\ln(m_H^2)\right. \\
& \left. + \frac{21}{8}\ln(m_Z^2) + \frac{225}{16}\ln(m_H^2)\right] + z_H^2\left[-\frac{529}{48}\ln(m_Z^2) - \frac{295}{96}\ln(m_H^2) - \frac{45}{16}\ln(m_Z^2)\ln(m_H^2) - \frac{391}{384} + \frac{43}{32}\ln(m_Z^2)^2 + \frac{81}{16}\ln(m_H^2)^2\right. \\
& \left. + \frac{127}{16}\zeta_2 + 114S_2\right] + z_H^3\left[-\frac{1759}{96}\ln(m_Z^2) - \frac{1213}{96}\ln(m_H^2) - \frac{17}{4}\ln(m_H^2)^2 - \frac{23}{8}\ln(m_Z^2)^2 + \frac{59}{8}\ln(m_Z^2)\ln(m_H^2) + \frac{38687}{1152}\right. \\
& \left. + \frac{987}{16}S_2 - 7\zeta_2\right] + z_H^4\left[-\frac{16447}{480}\ln(m_H^2) - \frac{257}{8}\zeta_2 - \frac{63}{2}\ln(m_Z^2)^2 - \frac{255}{16}\ln(m_H^2)^2 - \frac{5033}{480}\ln(m_Z^2) + \frac{759}{16}\ln(m_Z^2)\ln(m_H^2)\right. \\
& \left. + \frac{1948279}{28800} + \frac{11559}{32}S_2\right] + z_H^5\left[-\frac{3573}{16}\zeta_2 - \frac{2775}{16}\ln(m_Z^2)^2 - \frac{1761}{16}\ln(m_H^2)^2 - \frac{142399}{3360}\ln(m_H^2) - \frac{92381}{3360}\ln(m_Z^2)\right. \\
& \left. + \frac{108755447}{470400} + \frac{567}{2}\ln(m_Z^2)\ln(m_H^2) + \frac{40827}{32}S_2\right],
\end{aligned}$$

$$R_3^{\overline{\rm MS}}=\left[-\frac{243}{8}S_2-\frac{27}{2}\ln(m_H^2)+\frac{27}{8}\ln(m_H^2)^2+\frac{457}{32}+\zeta_2\right]+z_H\left[-\frac{2315}{128}-\frac{243}{32}S_2-\frac{99}{16}\zeta_2-\frac{63}{16}\ln(m_H^2)^2-\frac{45}{16}\ln(m_Z^2)\ln(m_H^2)\right.$$
$$+\frac{105}{32}\ln(m_Z^2)+\frac{1083}{64}\ln(m_H^2)\Big]+z_H^2\Big[-\frac{2161}{192}\ln(m_Z^2)-\frac{179}{48}\ln(m_H^2)+\frac{67}{32}\ln(m_Z^2)^2+\frac{233}{32}\ln(m_H^2)^2+\frac{333}{32}S_2+\frac{257}{16}\zeta_2$$
$$+\frac{25579}{1152}-5\ln(m_Z^2)\ln(m_H^2)\Big]+z_H^3\Big[-\frac{629}{32}\ln(m_H^2)-\frac{375}{32}S_2-\frac{113}{16}\zeta_2-\frac{145}{32}\ln(m_H^2)^2-\frac{93}{32}\ln(m_Z^2)^2+\frac{171}{32}\ln(m_Z^2)$$
$$+\frac{127}{16}\ln(m_Z^2)\ln(m_H^2)+\frac{13183}{576}\Big]+z_H^4\Big[-\frac{657}{16}S_2-\frac{7789}{480}\ln(m_H^2)-\frac{11}{4}\ln(m_Z^2)^2-\frac{11}{4}\ln(m_H^2)^2+\frac{11}{2}\ln(m_Z^2)\ln(m_H^2)$$
$$+\frac{3047}{240}\ln(m_Z^2)+\frac{497737}{28800}-6\zeta_2\Big]+z_H^5\Big[-\frac{17787}{32}S_2-\frac{1571}{16}\ln(m_Z^2)\ln(m_H^2)-\frac{97161}{1120}\ln(m_H^2)-\frac{41295691}{1411200}+\frac{609}{16}\ln(m_H^2)^2$$
$$+\frac{481}{8}\ln(m_Z^2)^2+\frac{1219}{16}\zeta_2+\frac{55681}{420}\ln(m_Z^2)\Big],$$

$$R_4^{\overline{\rm MS}}=\left[-\frac{1215}{32}S_2-\frac{135}{8}\ln(m_H^2)+\frac{5}{4}\zeta_2+\frac{135}{32}\ln(m_H^2)^2+\frac{2285}{128}\right]+z_H\left[-\frac{6817}{320}-\frac{243}{32}S_2-\frac{117}{16}\zeta_2-\frac{9}{2}\ln(m_H^2)^2\right.$$
$$-\frac{27}{8}\ln(m_Z^2)\ln(m_H^2)+\frac{63}{16}\ln(m_Z^2)+\frac{3153}{160}\ln(m_H^2)\Big]+z_H^2\Big[-\frac{1347}{32}S_2-\frac{349}{30}\ln(m_Z^2)-\frac{115}{16}\ln(m_Z^2)\ln(m_H^2)-\frac{851}{192}\ln(m_H^2)$$
$$+\frac{91}{32}\ln(m_Z^2)^2+\frac{19}{2}\ln(m_H^2)^2+\frac{171}{8}\zeta_2+\frac{51769}{1440}\Big]+z_H^3\Big[-\frac{1243}{48}\ln(m_H^2)-\frac{55}{4}S_2-\frac{53}{8}\zeta_2-\frac{77}{16}\ln(m_H^2)^2-\frac{47}{16}\ln(m_Z^2)^2+\frac{311}{40}$$
$$+\frac{17}{2}\ln(m_Z^2)\ln(m_H^2)+\frac{883}{60}\ln(m_Z^2)\Big]+z_H^4\Big[-\frac{2897}{192}\ln(m_H^2)-\frac{15}{16}\zeta_2-\frac{17}{32}S_2-\frac{15}{32}\ln(m_Z^2)^2-\frac{15}{32}\ln(m_H^2)^2+\frac{15}{16}\ln(m_Z^2)\ln(m_H^2)$$
$$+\frac{38587}{14400}+\frac{1013}{192}\ln(m_Z^2)\Big]+z_H^5\Big[-\frac{1366523}{33600}-\frac{179}{8}\ln(m_Z^2)\ln(m_H^2)-\frac{3497}{160}\ln(m_H^2)+\frac{179}{16}\ln(m_Z^2)^2+\frac{179}{16}\ln(m_H^2)^2$$
$$+\frac{1281}{80}\ln(m_Z^2)+\frac{183}{8}\zeta_2+\frac{791}{16}S_2\Big],$$

$$R_5^{\overline{\rm MS}}=\left[-\frac{729}{16}S_2-\frac{81}{4}\ln(m_H^2)+\frac{3}{2}\zeta_2+\frac{81}{16}\ln(m_H^2)^2+\frac{1371}{64}\right]+z_H\left[-\frac{7829}{320}-\frac{135}{16}\zeta_2-\frac{243}{32}S_2-\frac{81}{16}\ln(m_H^2)^2-\frac{63}{16}\ln(m_Z^2)\ln(m_H^2)\right.$$
$$+\frac{147}{32}\ln(m_Z^2)+\frac{3591}{160}\ln(m_H^2)\Big]+z_H^2\Big[-\frac{24949}{288}S_2-\frac{1931}{160}\ln(m_Z^2)-\frac{75}{8}\ln(m_Z^2)\ln(m_H^2)-\frac{497}{96}\ln(m_H^2)+\frac{115}{32}\ln(m_Z^2)^2$$
$$+\frac{375}{32}\ln(m_H^2)^2+\frac{419}{16}\zeta_2+\frac{12475499}{259200}\Big]+z_H^3\Big[-\frac{641}{20}\ln(m_H^2)-\frac{3211}{288}S_2-\frac{99}{16}\zeta_2-\frac{163}{32}\ln(m_H^2)^2-\frac{34321}{10368}-\frac{95}{32}\ln(m_Z^2)^2$$
$$+\frac{145}{16}\ln(m_Z^2)\ln(m_H^2)+\frac{20329}{960}\ln(m_Z^2)\Big]+z_H^4\Big[-\frac{4799}{240}\ln(m_H^2)-\frac{29}{8}\ln(m_Z^2)\ln(m_H^2)+\frac{113273}{259200}+\frac{29}{16}\ln(m_Z^2)^2+\frac{29}{16}\ln(m_H^2)^2$$
$$+\frac{343}{144}S_2+\frac{29}{8}\zeta_2+\frac{1363}{192}\ln(m_Z^2)\Big]+z_H^5\Big[-\frac{57473}{960}\ln(m_H^2)-\frac{321}{8}\ln(m_Z^2)\ln(m_H^2)-\frac{39526351}{1814400}+\frac{97}{36}S_2+\frac{321}{16}\ln(m_Z^2)^2$$
$$+\frac{321}{16}\ln(m_H^2)^2+\frac{321}{8}\zeta_2+\frac{5627}{96}\ln(m_Z^2)\Big].$$

APPENDIX E: MASS DIFFERENCE EXPANSION OF $\Delta r_{\rm bos}^{(2)}$ IN THE $\overline{\rm MS}$ SCHEME

The correction in the $\overline{\rm MS}$ scheme is given by six coefficients in the double expansion in the mass differences between the W and Z bosons and between the Higgs boson and the Z bosons:

$$(\Delta r^{(2)}_{\rm bos})^{\overline{\rm MS}} = \left(\frac{\alpha}{4\pi \sin^2\theta_W}\right)^2 \sum_{n=0}^{5} \sin^{2n}\theta_W R_n^{\overline{\rm MS}}. \tag{E1}$$

All parameters are in the $\overline{\rm MS}$ scheme and $h_Z=(m_H^2-m_Z^2)/m_Z^2$. Note also that the logarithms contain the renormalization scale as $\ln(m_Z^2)=\ln(m_Z^2/\mu^2)$:

$$\begin{aligned}
R_0^{\overline{\rm MS}} =& \left[-\frac{3673}{48}+\frac{15}{16}\zeta_2+\frac{7749}{32}S_2+\frac{389}{4}\ln(m_Z^2)-\frac{45}{2}\ln(m_Z^2)^2\right]+h_Z\left[+\frac{37739}{576}-\frac{23}{4}\zeta_2-\frac{4053}{16}S_2-\frac{4345}{48}\ln(m_Z^2)\right.\\
&\left.+\frac{489}{16}\ln(m_Z^2)^2\right]+h_Z^2\left[-\frac{66773}{1152}+\frac{7}{4}\zeta_2+\frac{9083}{32}S_2+\frac{6857}{96}\ln(m_Z^2)-\frac{1005}{32}\ln(m_Z^2)^2\right]+h_Z^3\left[+\frac{93671}{1728}-3\zeta_2-\frac{14509}{48}S_2\right.\\
&\left.-\frac{26611}{480}\ln(m_Z^2)+\frac{129}{4}\ln(m_Z^2)^2\right]+h_Z^4\left[-\frac{829957}{17280}+3\zeta_2+\frac{7321}{24}S_2+\frac{35641}{960}\ln(m_Z^2)-\frac{129}{4}\ln(m_Z^2)^2\right]\\
&+h_Z^5\left[+\frac{7597621}{181440}-3\zeta_2-\frac{44257}{144}S_2-\frac{29863}{1680}\ln(m_Z^2)+\frac{129}{4}\ln(m_Z^2)^2\right],
\end{aligned}$$

$$\begin{aligned}
R_1^{\overline{\rm MS}} =& \left[+\frac{1325}{36}-\frac{17}{4}\zeta_2-\frac{4119}{8}S_2-\frac{321}{4}\ln(m_Z^2)+\frac{43}{2}\ln(m_Z^2)^2\right]+h_Z\left[-\frac{1333}{96}+\frac{9}{4}\zeta_2+\frac{1685}{4}S_2+\frac{915}{16}\ln(m_Z^2)-\frac{181}{8}\ln(m_Z^2)^2\right]\\
&+h_Z^2\left[+\frac{18011}{576}-2\zeta_2-\frac{1929}{4}S_2-\frac{4013}{80}\ln(m_Z^2)+\frac{371}{16}\ln(m_Z^2)^2\right]+h_Z^3\left[-\frac{630583}{17280}+2\zeta_2+\frac{2713}{6}S_2+\frac{31199}{960}\ln(m_Z^2)\right.\\
&\left.-\frac{43}{2}\ln(m_Z^2)^2\right]+h_Z^4\left[+\frac{79808347}{1814400}-2\zeta_2-\frac{64831}{144}S_2-\frac{56941}{3360}\ln(m_Z^2)+\frac{43}{2}\ln(m_Z^2)^2\right]\\
&+h_Z^5\left[-\frac{95205863}{1814400}+2\zeta_2+\frac{16235}{36}S_2+\frac{2561}{960}\ln(m_Z^2)-\frac{43}{2}\ln(m_Z^2)^2\right],
\end{aligned}$$

$$\begin{aligned}
R_2^{\overline{\rm MS}} =& \left[+\frac{1519}{72}-\frac{3}{16}\zeta_2+\frac{1671}{32}S_2-\frac{607}{12}\ln(m_Z^2)+\frac{3}{4}\ln(m_Z^2)^2\right]+h_Z\left[-\frac{21679}{864}+\frac{3}{4}\zeta_2-\frac{541}{24}S_2+\frac{27307}{480}\ln(m_Z^2)\right.\\
&\left.-\frac{13}{16}\ln(m_Z^2)^2\right]+h_Z^2\left[+\frac{889057}{25920}+\frac{7}{4}\zeta_2-\frac{20549}{288}S_2-\frac{79529}{960}\ln(m_Z^2)+\frac{89}{32}\ln(m_Z^2)^2\right]+h_Z^3\left[-\frac{11857673}{453600}-\zeta_2+\frac{1073}{36}S_2\right.\\
&\left.+\frac{313069}{3360}\ln(m_Z^2)-\frac{1}{4}\ln(m_Z^2)^2\right]+h_Z^4\left[+\frac{4154501}{272160}+\zeta_2-\frac{5905}{432}S_2-\frac{356431}{3360}\ln(m_Z^2)+\frac{1}{4}\ln(m_Z^2)^2\right]+h_Z^5\left[-\frac{1060729937}{114307200}\right.\\
&\left.-\zeta_2+\frac{10309}{648}S_2+\frac{270507}{2240}\ln(m_Z^2)-\frac{1}{4}\ln(m_Z^2)^2\right],
\end{aligned}$$

$$\begin{aligned}
R_3^{\overline{\rm MS}} =& \left[+\frac{5707}{108}+\frac{21}{4}\zeta_2-\frac{1325}{12}S_2-\frac{1223}{40}\ln(m_Z^2)+\frac{3}{2}\ln(m_Z^2)^2\right]+h_Z\left[-\frac{1230667}{25920}+\frac{5}{4}\zeta_2+\frac{265}{36}S_2+\frac{13787}{480}\ln(m_Z^2)\right.\\
&\left.-\frac{1}{2}\ln(m_Z^2)^2\right]+h_Z^2\left[+\frac{66550571}{907200}+\frac{7}{2}\zeta_2-\frac{17893}{144}S_2-\frac{86971}{1680}\ln(m_Z^2)+\frac{31}{8}\ln(m_Z^2)^2\right]+h_Z^3\left[-\frac{13312007}{155520}-2\zeta_2\right.\\
&\left.+\frac{40147}{432}S_2+\frac{5683}{105}\ln(m_Z^2)-\frac{1}{2}\ln(m_Z^2)^2\right]+h_Z^4\left[+\frac{2337399703}{28576800}+2\zeta_2-\frac{33491}{648}S_2-\frac{42847}{720}\ln(m_Z^2)+\frac{1}{2}\ln(m_Z^2)^2\right]\\
&+h_Z^5\left[-\frac{374331501521}{4115059200}-2\zeta_2+\frac{43928}{729}S_2+\frac{2708207}{40320}\ln(m_Z^2)-\frac{1}{2}\ln(m_Z^2)^2\right],
\end{aligned}$$

$$R_4^{\overline{\rm MS}}=\left[+\frac{247637}{4320}+\frac{63}{8}\zeta_2-\frac{8731}{48}S_2-\frac{2503}{80}\ln(m_Z^2)+\frac{9}{4}\ln(m_Z^2)^2\right]+h_Z\left[-\frac{3817759}{100800}+\frac{7}{4}\zeta_2+\frac{67}{12}S_2+\frac{6661}{224}\ln(m_Z^2)\right.$$
$$\left.-\frac{3}{16}\ln(m_Z^2)^2\right]+h_Z^2\left[+\frac{329665169}{5443200}+\frac{21}{4}\zeta_2-\frac{111709}{864}S_2-\frac{66001}{1120}\ln(m_Z^2)+\frac{159}{32}\ln(m_Z^2)^2\right]+h_Z^3\left[-\frac{803801701}{9525600}-3\zeta_2\right.$$
$$\left.+\frac{28865}{216}S_2+\frac{1256243}{20160}\ln(m_Z^2)-\frac{3}{4}\ln(m_Z^2)^2\right]+h_Z^4\left[+\frac{275880109013}{4115059200}+3\zeta_2-\frac{276031}{5832}S_2-\frac{2789701}{40320}\ln(m_Z^2)\right.$$
$$\left.+\frac{3}{4}\ln(m_Z^2)^2\right]+h_Z^5\left[-\frac{199097721241}{2514758400}-3\zeta_2+\frac{96601}{1296}S_2+\frac{17481691}{221760}\ln(m_Z^2)-\frac{3}{4}\ln(m_Z^2)^2\right],$$

$$R_5^{\overline{\rm MS}}=\left[+\frac{1180117}{18144}+10\zeta_2-\frac{17483}{72}S_2-\frac{58129}{1680}\ln(m_Z^2)+3\ln(m_Z^2)^2\right]+h_Z\left[-\frac{49494491}{1360800}+\frac{9}{4}\zeta_2+\frac{1651}{216}S_2+\frac{111187}{3360}\ln(m_Z^2)\right.$$
$$\left.+\frac{1}{8}\ln(m_Z^2)^2\right]+h_Z^2\left[+\frac{973643677}{19051200}+7\zeta_2-\frac{12185}{108}S_2-\frac{230051}{3360}\ln(m_Z^2)+\frac{97}{16}\ln(m_Z^2)^2\right]+h_Z^3\left[-\frac{405345006701}{4115059200}-4\zeta_2\right.$$
$$\left.+\frac{1116793}{5832}S_2+\frac{195907}{2688}\ln(m_Z^2)-\ln(m_Z^2)^2\right]+h_Z^4\left[+\frac{2758671944087}{45265651200}+4\zeta_2-\frac{78913}{2916}S_2-\frac{6006071}{73920}\ln(m_Z^2)+\ln(m_Z^2)^2\right]$$
$$+h_Z^5\left[-\frac{33815515952111}{407390860800}-4\zeta_2+\frac{1210235}{13122}S_2+\frac{3432923}{36960}\ln(m_Z^2)-\ln(m_Z^2)^2\right].$$

[1] Particle Data Group, K. Hagiwara *et al.*, Phys. Rev. D **66**, 010001 (2002).

[2] ATLAS Collaboration, Report No. CERN/LHCC/99-15, 1999; CMS Collaboration, Report No. CMS TDR 1–5, 1997/98; S. Haywood *et al.*, hep-ph/0003275.

[3] TESLA Technical Design Report, Part III, edited by R. Heuer, D.J. Miller, F. Richard, and P.M. Zerwas, DESY-2001-11C, hep-ph/0106315; T. Abe *et al.*, hep-ex/0106057.

[4] G. Degrassi, P. Gambino, and A. Vicini, Phys. Lett. B **383**, 219 (1996); **394**, 188 (1997); A. Freitas, W. Hollik, W. Walter, and G. Weiglein, *ibid.* **495**, 338 (2000).

[5] A. Freitas, W. Hollik, W. Walter, and G. Weiglein, Nucl. Phys. **B632**, 189 (2002).

[6] M. Awramik and M. Czakon, Phys. Rev. Lett. **89**, 241801 (2002).

[7] A. Onishchenko and O. Veretin, Phys. Lett. B **551**, 111 (2003).

[8] S.M. Berman, Phys. Rev. **112**, 267 (1958); T. Kinoshita and A. Sirlin, *ibid.* **113**, 1652 (1959).

[9] T. van Ritbergen and R.G. Stuart, Phys. Rev. Lett. **82**, 488 (1999).

[10] A. Sirlin, Phys. Rev. D **22**, 971 (1980).

[11] A. Sirlin, Phys. Rev. D **29**, 89 (1984).

[12] S.G. Gorishnii, Nucl. Phys. **B319**, 633 (1989).

[13] F.V. Tkachov, Report No. INR P-0332, Moscow, 1983; Report No. P-0358, Moscow, 1984; K.G. Chetyrkin, Theor. Math. Phys. **75**, 26 (1988); **76**, 207 (1988); Report No. MPI-PAE/PTh-13/91, Munich, 1991; V.A. Smirnov, Commun. Math. Phys. **134**, 109 (1990); *Renormalization and Asymptotic Expansions* (Birkhäuser, Basel, 1991); *Applied Asymptotic Expansions in Momenta and Masses*, Springer Tracts in Modern Physics Vol. 177 (Springer, Berlin, 2002).

[14] N.N. Bogolyubov and D.V. Shirkov, *Introduction to the Theory of Quantized Fields*, Interscience Monographs in Physics and Astronomy, Vol. 3 (Wiley, New York, 1959).

[15] A.I. Davydychev and J.B. Tausk, Nucl. Phys. **B397**, 123 (1993).

[16] F.V. Tkachov, Phys. Lett. **100B**, 65 (1981); K.G. Chetyrkin and F.V. Tkachov, Nucl. Phys. **B192**, 159 (1981).

[17] T. Appelquist, J. Carazzone, T. Goldman, and H.R. Quinn, Phys. Rev. D **8**, 1747 (1973).

[18] J.C. Taylor, *Gauge Theories Of Weak Interactions* (Cambridge University Press, Cambridge, England, 1976); J. Fleischer and F. Jegerlehner, Phys. Rev. D **23**, 2001 (1981).

[19] F. Jegerlehner, M.Y. Kalmykov, and O. Veretin, Nucl. Phys. **B641**, 285 (2002).

[20] P. Breitenlohner and D. Maison, Commun. Math. Phys. **52**, 11 (1977).

[21] P. Gambino and P.A. Grassi, Phys. Rev. D **62**, 076002 (2000).

[22] K.I. Aoki, Z. Hioki, M. Konuma, R. Kawabe, and T. Muta, Prog. Theor. Phys. Suppl. **73**, 1 (1982).

[23] S. Bauberger, Doctoral thesis, University of Würzburg, 1997.

[24] D.J. Gross and F. Wilczek, Phys. Rev. D **8**, 3633 (1973).

[25] D.R.T. Jones, Nucl. Phys. **B87**, 127 (1975); Phys. Rev. D **25**, 581 (1982); M.E. Machacek and M.T. Vaughn, Nucl. Phys. **B222**, 83 (1983).

[26] M. Czakon (in preparation).

[27] M. Tentyukov and J. Fleischer, Comput. Phys. Commun. **132**, 124 (2000).

[28] G. Weiglein, R. Scharf, and M. Bohm, Nucl. Phys. **B416**, 606 (1994).

[29] S. Bauberger and M. Bohm, Nucl. Phys. **B445**, 25 (1995).

[30] S. Bauberger, ftp://ftp.physik.uni-wuerzburg.de/pub/hep/index.html
[31] M.J. Veltman, Acta Phys. Pol. B **8**, 475 (1977).
[32] J.A. Vermaseren, math-ph/0010025.
[33] N. Gray, D.J. Broadhurst, W. Grafe, and K. Schilcher, Z. Phys. C **48**, 673 (1990).
[34] J. Fleischer and M.Yu. Kalmykov, Comput. Phys. Commun. **128**, 531 (2000).